Permission to Build: Climate Risk and Property Tax Revenue *

Qianping Ren †

January 2025

Abstract

Private market failures lead to over-development of houses in climate risky areas. This paper examines the impact of state-level building codes on housing development in wildfire-prone areas of California using a spatial regression discontinuity design around the regulatory boundaries. I find a significant decrease in housing development and taxable property value in regulated areas. Local governments, who are responsible for designing and implementing climate adaptation strategies, have a perverse incentive to gain property tax revenue that distorts their decisions, necessitating a central regulation. I propose a conceptual model to illustrate the theoretical concern and empirically test it. I find that the reductions are larger in local jurisdictions with higher dependency on property tax revenue. The results generally shed light on the challenges of climate adaptation (e.g. managed retreat) where property tax incentives may create inefficient local government policies to correct housing market failures.

JEL: D62, H12, Q54, Q58, R31, R51

Keywords: climate risk, property tax, fire hazard severity, housing development, building codes, risk management

1 Introduction

From 1980 to 2023, 376 weather and climate disasters occurred in the US, with cumulative cost exceeding 2.7 trillion dollars (NOAA National Centers for Environmental Information, 2024a). In 2021 alone, nearly 15 million homes in the US were affected by climate disasters. The frequency, intensity and cost of extreme natural disasters are increasing and expected to accelerate (Coronese et al., 2019). Extreme weather events has lead as the top risk over the next decade (World Economic Forum, 2024). There are two main reasons for the increasing severity, exposure and vulnerability. The first is the increasing climate change (Coronese et al., 2019). The second is the rapidly growing residential development in high climate risk areas (Mann et al., 2014; Katz and Marr, 2022). For example, over 115 million people and 48 million buildings (both are about one-third of the national totals) in the US are living in areas with high wildfire risk (wildfirerisk.org, 2024). Up to 1.7 million homes will be within the very high fire hazard severity zone by 2050 (Mann et al., 2014).

Why do people keep building in climate risky areas? The reasons can be attributed to private market failures. First, developers may misperceive climate risk level (McCoy and Walsh, 2018). Second, they may ignore the spatial positive/negative externality to neighborhoods (Shafran, 2008). For example, when a fire occurs, the burning of the house will put the neighboring houses in danger. Third, moral hazard from public spending programs (Baylis and Boomhower, 2023). Fourth, the imperfect insurance market (Wagner, 2022). These lead developers disproportionately to over-develop among these high-risk parcels, compared to the social optimal level. Theoretically, these private market failures can be fully corrected by governments if they act effectively.

This paper empirically investigates the impact of state-level building codes on housing development in wildfire-prone areas of California, the US. The regulation provides a natural quasi-experiment by designating the Very High Fire Hazard Severity Zone (VHFHSZ) maps, where the wildfire risk is very high according to scientific model simulations. The Bates Bill of 1992 (Assembly Bill 337) requires the California Department of Forestry and Fire Protection (CAL FIRE) to identify and produce recommended fire hazard severity zones (FHSZ) maps within the state. In local responsibility areas (LRA), VHFHSZ maps are recommended.[1] Housing development within VHFHSZ is required to follow stricter building

---

[1]Local responsibility areas (LRA) are the areas that the local government is responsible for wildfire protection. They include incorporated cities, urban regions, agriculture lands, and portions of the desert. Fire protection is typically provided by city fire departments, fire protection districts, counties, and by CAL FIRE under contract to local government.

codes (e.g. fire-resistant building materials and methods, maintaining 100 feet defensible space around houses). The drawing of the maps is arguably exegoneous as CAL FIRE states that they are based on a geospatial model with inputs such as vegetation type, slope, wind, and fire history.[2] I apply a spatial regression discontinuity design (SRDD) around the hazard zone boundary. The main results indicate a 0.006 houses reduction per $30{\times}30$m pixel. This reduction is 22.2% of the mean level of development in the analysis sample, and is equal to 67 houses per 10 km^2. The estimate in taxable property value suggests a 9.3% reduction per pixel within VHFHSZ, which is 32.0% of the mean value in our sample.

The SRDD replies on that other factors determining real estate development move smoothly across the boundaries. I validate this assumption by collecting granular data on land pixels, parcels, house characteristics, terrain characteristics and road network, and performing four identification tests. First, if there are some other factors determining real estate development and they are correlated with the boundary designation, then there could be some discontinuity around the boundary before the map release in 2008. Using parcels developed during pre map period, I find no significant discontinuity around the boundary. Second, I find that the terrain characteristics, including slope, roughness and Terrain Ruggedness Index move smoothly across the boundaries. Third, infrastructure construction could bring additional and uneven effects on nearby neighborhoods (Gonzalez-Navarro and Quintana-Domeque, 2016). If infrastructure construction overlaps the boundary, then the true effects could be confounded. One particularly important infrastructure in US is road. To test this, I collect the road network data in major counties in California, and find only 10.16% of the boundary are within 50 meters of the roads. Furthermore, the distribution of the distance from the zone boundary to the roads is generally uniform. Fourth, I perform a permutation test proposed by Ganong and Jäger (2018). By moving the boundary further outside the "true" boundary at a 30m interval till 180m, I perform the estimation using the same SRDD regression specification. These placebo estimates are much smaller than the true estimate, and nearly all of them are statistically insignificant. Therefore, based on the identification test results, it's unlikely our true estimates are driven by other factors other than the regulation itself.

However, practically, local governments are the root and frontiers of climate adaptation policy design and implementation. They have strong discretion of power to address and

---

[2]Appendix C prvoides the method details on how the zones are drawn and classified. Original sources: https://osfm.fire.ca.gov/what-we-do/community-wildfire-preparedness-and-mitigation/fire-hazard-severity-zones. There is also a YouTube video produced by CAL FIRE: https://www.youtube.com/watch?v=oXwnUCFVGxI.

adapt to the increasing climate risk and responsible for putting building codes and permitting house constructions. The state-level regulation would be unnecessary or have null effects if local governments act effectively in correcting the private market failures. Why not then? The situation is that the local governments face a trade-off between restricting housing development in climate risky areas, thus reducing the risk exposure and the potential damage if there is a climate disaster, and capturing more property tax revenue generated in these climate risky areas. Two stylized facts strength the property tax revenue incentive for the local governments. First, property tax is an important source of government budget, particularly for local governments (counties, cities, school districts, and special districts). The average property tax rate in local jurisdictions is around 1.5% (Harris et al., 2013). Property tax revenues are more than $62.1 billion for fiscal year 2016-2017 in California (California State Board of Equalization, 2018).[3] Second, climate risk and property value are positively correlated, and furthermore the correlation is potentially disproportionate. Figure 1 presents the correlation between wildfire risk and property value in Los Angeles County, CA. We can observe a significant positive correlation. Particularly, areas with highest risk have disproportionate high property value.

I propose a conceptual model to illustrate this political economy concern and empirically test it. By combining the main data with the public finance census data at local government level before the map release, I find that both estimates are larger in local jurisdictions with high dependency on property tax revenue compared to other sources of revenue, and much smaller and statistically insignificant in local jurisdictions with low dependency. The findings are consistent with the model predictions, and support that the property tax revenue incentive is likely an important problem distorting the optimal decisions of the local governments.

To gain a comprehensive understanding of the regulation's overall reduction effects, I expand the boundary estimates to include the inner-zone areas. Some coarse extrapolations suggest that if the estimate on housing development is extrapolated to 1 km distance inside the zone boundary, it indicates that around thirteen thousands of houses are less constructed within this area. At the extreme, given that there are around 3495 km^2 VHFHSZ in California, the estimate indicates that because of the regulation, 23,297 fewer houses are built.

---

[3]Particularly, Proposition 13, which was effective in 1978, strictly constrains the property tax collection by limiting the property tax rate to 1 percent and the further tax increases. This leads to a huge decrease of property tax revenue in the following years. Figure A3 (a) presents the property tax revenue trend for years 1970-2019. This constraint also intensifies the incentive to increase the tax base for local governments in California.

Following similar deduction logic, the estimate on taxable property value indicates that around 1.03 billion dollars are lost within 1 km distance inside the zone boundary. Again, if extrapolated to all VHFHSZ in California, it leads to around 1.7 billion dollars reduction in taxable property value. Given that the average property tax rate is 1.5%, then it indicates a 26 million dollars property tax revenue reduction. Furthermore, considering the housing is a stock, while the property value is just flow, a net present value using a discount rate of 2%, which is the constraint rate set by Proposition 13 in California, indicates that the reduction of property tax revenue will be nearly 1 billion dollars. This is about 60 times of the average local property tax revenue in 2019.

This paper contributes to several strands of the literature. First and most directly, this paper provides new evidence about the regulation of wildfire building codes, particularly the Fire Hazard Severity Zone (FHSZ) regulations. Several concurrent studies investigate the salience of risk on house prices based on FHSZ (Garnache, 2023; Ma et al., 2024) with the focus on State Responsibility Areas (SRA). While this paper focuses on LRA, where local governments play an important role in climate adaptation. Importantly, the impacts on housing development and property tax revenue have not been studied yet. This paper contributes to a growing literature on the determinants of housing development. Previous literature explores other determinants, such as natural resources and terrain characteristics (Burchfield et al., 2006; Saiz, 2010), sea level rise risk (Lin et al., 2024), other types of land use regulations (Mayer and Somerville, 2000), particularly minimum lot size restrictions, (e.g. Glaeser and Ward, 2009; Song, 2021; Gyourko and McCulloch, 2023), and environmental policies (e.g. Ren and West, 2023a; Li et al., 2024). The relationship between property tax and urban/suburban development mainly focuses on whether a higher property tax increases or decreases urban sprawl and the results are quite mixed (e.g. Brueckner and Kim, 2003; Song and Zenou, 2006; Lutz, 2015; Wassmer, 2016).[4] This paper takes a different perspective on this topic by arguing that the taxable property value incentive itself rather than the property tax rate could also distort housing development and how this distortion is corrected by central government regulations.

---

[4]Brueckner and Kim (2003) investigate the relationship between property tax and urban sprawl, and argue that there are two countervailing effects of property tax on the sprawl level: improvements effect, where the property tax induces lower density and encourages city expansion; dwelling-size effect, where the property tax decreases the dwelling size, thus increasing population density and pressuring down the city size. Empirically, they find that the property tax leads to an efficient expansion of cities. However, Song and Zenou (2006) find an opposite result based on 448 urbanized areas in the US. Lutz (2015) uses a quasi-natural shock to property tax burden in New Hampshire, US and finds that a reduced property tax substantially increases house construction.

Second, this study also joins a growing and significant literature on the impacts of governmental natural disaster management policies and how these policies could even distort the optimal adaptation. The polices include floodplain maps (Hino and Burke, 2021; Ostriker and Russo, 2024), wildfire building codes (Baylis and Boomhower, 2022), and infrastructure construction (Hsiao, 2023; Balboni, 2025). For example, a proposed sea wall to combat sea level rise in Jakarta creates coastal lock-in by encouraging new coastal development, which brings substantial welfare losses (Hsiao, 2023). This adaptation-misleading policies also happened and created losses in Vietnam by persistent coastal investment favoritism (Balboni, 2025) and in the US by non-optimal regulatory commitment (Lim and Yurukoglu, 2018) and by increasing wildfire firefighting expenditures (Baylis and Boomhower, 2023). This paper goes further by investigating how central government regulations can address the distortions caused by local government policies that are misaligned with effective adaptation, driven by incentives related to property tax revenue.

Finally, this paper broadly speaks to how the level of government matters for correcting for market failures. Federal policies could discourage the state-level correction efforts (Knight, 2002), and state agencies could be more effective in correcting than federal governments (Jung and Makowsky, 2014). This paper provides novel evidence in two parts: I focus on two different levels of government, the state and local agencies; I focus on the property tax incentive discrepancy at the two levels of governments. More generally, the study is also related to the different preferences on regulation across the multiple levels of governments and their interactions (Ren and West, 2023b; Anders and Campbell, 2024).

The remainder of the paper is structured as follows. Section 2 introduces the background of wildfires, property tax and local public finance in the US, and VHFHSZ and the related building codes requirement. Section 3 develops a conceptual framework to model how local governments create a market failure by the incentive of gaining more property tax revenue and how the central regulation corrects this failure. Section 4 describes the data used in the analysis, and Section 5 outlines the empirical strategy. Section 6 presents the main results on housing development and property tax revenue, robustness checks and heterogeneous analysis. Section 7 concludes.

2 Background

2.1 Increasing Wildfire Trend and Cost

Wildfire is widespread and with an increasing severity in US, especially western states, e.g. California. Nine of the top 10 Largest wildfires in California are in the recent decade. Wildfire burned 10.1 million acres in 2020, over four times the 2.4 million acres in 1987 (National Interagency Fire Center, 2022). Figure A1 presents the trends on acres burned in California and the US. An observed stylized fact is that there has been an even stronger increasing trend in the recent decade.

Huge and increasing damage is caused by wildfires. 5,972 structures were burned because of wildfires in 2021 (Congressional Research Service, 2023). The number is expected to increase to 17,139 anually in the current environment, and could grow to around 33,753 in the next thirty years (First Street Foundation, 2023). The economic losses from wildfires is 182.4 billion dollars (CPI-adjusted) from 1980 to 2023 in the US (NOAA National Centers for Environmental Information, 2024b).

2.2 Very High Fire Hazard Severity Zone and Regulations

The Oakland Hills Fire of 1991 destroyed 2,500 homes and killed 25 people. This prompted the mid-1990s Bates Bill (Assembly Bill 337), Government Code Section 51175, which requires CAL FIRE to evaluate fire hazard severity in LRA and recommend maps where very high FHSZs exist. The maps are not mandatory until the passing of S.B. 1260 in 2018, which redefines the VHFHSZ program in LRA as a state-mandated one, effective in 2019. When receiving the maps, local governments have 120 days to decide to accept or reject the maps. Once accepting the recommended maps from CAL FIRE, new developments or major retrofits in VHFHSZ are required to follow stricter building codes (Chapter 7A of the California Building Code), and all residents must comply with the defensible space requirements.

The first version of maps were released in 1998 by CAL FIRE. 209 cities were identified with VHFHSZ, of which only 99 adopted the maps. The second version of maps were released in 2008 and are based on updated scientific models, input data, and criteria. This version identified 188 cities with VHFHSZ. Unlike the first version, 173 cities (representing over 92% of the total) adopted or believed they had adopted this new version of maps (Miller et al.,

2020).[5]

This paper focuses on the second version of the maps in 2008.[6] There are two reasons for this. First, the high adoption of the maps, making selection bias at the local government level less concerned. Second, I am able to access the accurate Geographic Information System (GIS) data for the 2008 maps, while the data for the first edition cannot be accessed. Figure A2 (a) shows all LRAs and the 2008 VHFHSZs within LRA. Figure A2 (b) provides the VHFHSZ map for Los Angeles City. These VHFHSZ represent a total area of 3494.62 square kilometers and with a boundary length of about 8808 kilometers.[7]

2.3 Property Tax and Local Public Finance

Property tax is a major source of revenue for local governments in the US. Local governments include counties, municipalities (i.e., cities), townships, school districts, and special districts. Also, a major part of the public services is provided by local governments, such as public safety, education, public infrastructure (e.g. roads) and local amenities. These public goods are typically funded by local governments' own-source revenues, including taxes, fees, and charges. Of these, property tax is the largest source (Alm et al., 2014; Lincoln Institute of Land Policy and Minnesota Center for Fiscal Excellence, 2023). It makes up 73.5 percent of local own-source revenue (Barnett et al., 2014). This share can be even higher in high climate risk jurisdictions and has increased over time because of the reducing federal and state transfer to local governments (Shi and Varuzzo, 2020). Figure A3 (a) presents the property tax revenue trend for California local governments.

Although property tax is a primary source of revenue for local governments, that's not the case for state governments. For example, in California, the only property tax that is collected by the state government is on privately owned railroad cars, which is just a tiny portion of the total tax revenue of the state government. For state governments, they rely

---

[5]According to Meier et al. (2023)'s investigation, cities may consider this recommended maps mandatory, rather than optional. This is embodied in some city documents as well. For example, in a official document in Martinez City, Contra Costa County, it states "As a requirement of State law, the State Fire Marshal requires that each local jurisdiction which has areas identified as being within a Very High Fire Hazard Severity Zone (like Martinez) adopt an ordinance designating these areas in order to more accurately reflect the zones in Martinez that are susceptible to wildfire."

[6]2008 is a generally used time cutoff to indicate the map policy. While the posting time of the recommended maps from CAL FIRE varies across counties, ranging from May 2008 to November 2011.

[7]In the main analysis, I make one restriction on the boundary. I drop the boundaries which also serve as the boundary between Local Responsibility Areas (LRA) and State Responsibility Areas (SRA) since LRA and SRA are different types of areas as for firefighting responsibility, and other administrative responsibilities, which will potentially bias our estimates. This restriction reduces the length from 8808 km to 6418 km.

more on income taxes, sales taxes, and other excise taxes. Figure A3 (b) presents the total taxes, property taxes and sales taxes collected by the California state government from 1977 to 2019. Property tax represents only 3.6 percent of the total taxes, while sales tax makes up around 40 percent of the total amount.

This pattern creates a discrepancy in incentives for local governments and state governments. That is, local governments have an incentive to allow more constructions, particularly high market value ones, thus gaining higher property tax revenues. However, state governments do not have such an incentive.

3   Conceptual Framework

This section provides a conceptual and theoretical framework depicting how a market failure from the incentive of local governments to increase their property tax revenue fails to correct the private market failures, thus leads to over-development in areas with high climate risk (high-risk thereafter), and also how central government involvement, with no such a revenue incentive, corrects this local failure through regulation.[8] Local governments collect revenue from property tax and other taxes (e.g. sales tax). Among them, the property tax is a major source of funding for local jurisdictions. Local governments can take more property tax revenue by either increasing tax base or tax rate or both.[9]

I'll begin with a classic model of negative externality and how it is internalized through a Pigouvian tax by governments. Then I'll distinguish two level governments: local ones and the central one. The difference in property tax incentive between the local governments and the central government brings a market failure, which is from the incentive of local governments to increase their property tax revenue. Finally, I'll formalize how this additional market failure can be corrected by the central government, who doesn't have such a property tax revenue incentive.

---

[8]The theoretical framework constructed here is a static model, representing a process that is not simultaneously in reality. For example, homes aren't constructed at the same time, and property tax is a sequence of non-constant flows. However, the static model still captures the some key behavior incentive without loss of generality.

[9]In our empirical context of California, Proposition 13 , which was passed in 1978, further limits the capability of local governments to increase tax revenue by increasing tax rate. Proposition 13 limits the property tax rate to 1 percent and future property tax rate increases to 2 percent per year. This constraint intensifies the incentive of local governments to increase property tax revenue through the tax base channel.

3.1 Model Setup

In this model, we have developers and the government.[10] To simply, I assume that when developers decide to develop a property, there are always buyers consuming it. Or when there is a consumer demand, the developers will always satisfy it. This makes the model focus on the behaviors of developers and the government. Developers decide whether to develop a parcel into a property based on expected net profit. If yes, then they prepare and submit a construction plan to the government permitting office. The office reviews the plan and the relevant documents submitted and decides whether to approve or not. When approved, a building permit is issued. The government considers the general welfare of people and decides whether to correct any market failures when necessary.

Developer i faces a logit model problem.

$$\pi_i = (1 - t) * P_i - C_i \tag{1}$$

where t is the property tax rate. P_i is the price of the housing. C_i is the cost to own and develop the parcel, including the cost purchasing the land and the construction cost, but excluding the negative externality social cost. Developer i develops the parcel if $\pi_i > 0$, otherwise not.

3.2 Climate Risk, Externality and Building Regulation

The model focuses on areas with high climate risk, i.e. all of the parcels within the decision pool to the developer's choice is at high climate risk areas.[11] Climate risk in a parcel is positively associated with the level of negative externalities. The higher the risk, the higher social cost this externality brings to society. The externality could come from several sources. First, developers may misperceive climate risk level (McCoy and Walsh, 2018). Second, they may ignore the spatial negative externality to neighborhoods (Shafran, 2008). For example, when a fire occurs, the burning of the house will put the neighboring houses in danger. Third, moral hazard from public spending programs (Baylis and Boomhower, 2023). Fourth, the imperfect insurance market (Wagner, 2022). These lead developers disproportionately to over-develop among these high-risk parcels, compared to the social optimal level.

---

[10]For now, there is only one government. Later, the model will introduce two different levels of governments: local governments and the central government, where they have different incentives.

[11]This setting is consistent with the empirical part in this paper, where around the VHFHSZ boundary the wildfire risk is similarly high and moves smoothly.

Consider the developer's logit model problem with the social cost:

$$\pi_i = (1 - t) * P_i - C_i - C_i(\tau) \tag{2}$$

where the additional cost term $C_i(\tau)$ at the right-hand side is the social cost, which is positive. τ is the Pigouvian tax put by the government if there is any regulation to correct. In this model, I consider the form be building regulations and permitting cost set by the government. This induces an extra cost for developing.

The total amount of housing development in high risk areas is $Q = \sum_i I \{\pi_i\} > 0$. Without any correction, the optimal quantity is Q^*. With the Pigouvian correction, the optimal quantity developed is Q^o, which is the social optimal level. Figure A4 presents the two scenarios.

3.3 Market Failure in Local Governments

3.3.1 Model Setup in Local Governments

Now let's categorize the government into two different levels: the local governments and the central government. Practically, land planing and permitting is the responsibility of local governments, and property tax revenue is their major revenue source. The central government will only intervene when necessary. Local governments have an incentive to increase their revenue from property tax to maximize their net revenue.

$$\max_{Q_g} \psi + \rho(Q_g)(\psi + tQ_g) - G(Q_g) \tag{3}$$

where ψ is the tax revenue from other sources, e.g. sales tax, excise tax. $\rho(Q_g)$ measures the dependency on property tax revenue. t is the property tax rate. $G(Q_g)$ is the government expenditure for the housing development, mainly the public goods provision. g indicates a typical local government.

3.3.2 Market Failure in Housing Development at Local Governments

F.O.C of equation (3) w.r.t. Q_g, we have:

$$\rho'(Q_g^*)(\psi + Q_g^*) + \rho(Q_g^*)t = G'(Q_g^*) \tag{4}$$

To sustain a higher $\rho(Q_g^*)$, Q_g^* must be also larger. For simplicity of comparison, the local governments can be categorized into two types: High VS Low, based on the dependency on property tax revenue. For high dependency, the optimal quantity is denoted as Q_{gH}^*. For low dependency, the optimal quantity is denoted as Q_{gL}^*. Thus Q_g^* indicates the optimal quantity on an average dependency. Based on equation (4), the following ranking holds: $Q_{gL}^* < Q_g^* < Q_{gH}^*$.

If there is no property tax incentive, the local government will permit the social optimal quantity Q^o, where $Q^o < Q_g^*$. However, even with property tax incentive, the local government will not permit all high risk constructions, thus $Q_g^* < Q^*$.

3.4   Regulations by the Central Government

The central government doesn't have such an property tax incentive. The problem is:

$$\max \psi - G \tag{5}$$

Given that the central government doesn't have the property tax revenue incentive, it acts by correcting the private market failures, and moves the housing development quantity to Q^o.

3.5   Model Predictions

Integrating all of the four scenarios (Q_g^*, Q_{gH}^*, Q_{gL}^*, Q^o), figure A5 shows their relative rankings.

Then, the reduction effects of the regulation can be summarized as follows. The magnitude ranking is: Q_{gH}^* - Q^o < Q_g^* - Q^o < Q_{gL}^* - Q^o.

1. Overall effects: Q_g^* - Q^o.

2. High dependency: Q_{gH}^* - Q^o.

3. Low dependency: Q_{gL}^* - Q^o.

Verbally, then there are two predictions I can empirically test.

1. The central government regulations reduce building in climate risky areas.

2. This reduction in development reduces property tax revenue that local governments collect.

In the next sections, I casually test these two predictions in the context of wildfire risk and regulations in California using a spatial regression discontinuity design.

4 Data

I compile granular data on parcels with rich characteristics, building footprints, land covers, roads, terrain characteristics, and fire history in California. The analysis unit is 30×30m pixel. Data appendix B presents details on the data cleaning process.

4.1 VHFHSZ Maps and LRA

The maps are collected from CAL FIRE. CAL FIRE provides the high-resolution maps in both a pdf format and a Geographic Information System (GIS) shapefile format. For the maps, Very High Fire Hazard Severity Zones in the Local Responsibility Area are designated. Figure A2 (b) presents an example map of Los Angeles City. The GIS shapefile for LRA is also collected from CAL FIRE. This paper focuses on LRA, where the local government is responsible for wildfire protection. They include incorporated cities, urban regions, agriculture lands, and portions of the desert.

4.2 Land Cover Data

The land cover data comes from the National Land Cover Database (NLCD). NLCD is a national-wide geospatial database at high resolution (30×30m) provided by collaboration between the U.S. Geological Survey (USGS) and the Multi-Resolution Land Characteristics (MRLC) Consortium. The first version is in 1992, and then updated in 2001. Since then, it was regularly updated with an interval of 2-3 years. The newest version is 2021, released in July, 2023. I used the 2006 version since it is the closest edition before the VHFHSZ map release. This GIS data is in a raster format, with a land cover classification for each pixel.[12] I converted it to vector polygon data for further use. It also contains relevant terrain characteristics, including slope, Terrain Ruggedness Index, and roughness.[13] Figure

---

[12]There are eight broad classifications: water, developed, barren, forest, shrubland, herbaceous, planted/cultivated, and wetlands. Within each broad classification, there are more granular categories. For example, "water" is further classified into "open water" and "perennial ice/snow".

[13]Slope measures the angle of inclination of the terrain and is expressed in degrees. Terrain Ruggedness Index is a measurement of terrain heterogeneity, summarizing the change in elevation from the center to the surrounding cells. Roughness measures the degree of irregularity of the surface and is also computed from elevation.

A6 presents the raster maps of the whole contiguous nation and California using NLCD 2006 data. There are around 471 million 30×30m pixels in California in 2006.

4.3 Parcel Data

Parcel data provides detailed geolocation (polygons) and other characteristics of land lots. Each parcel is uniquely identified by an assessor's parcel number (APN). I collect these data from mainly two sources: public accessible sources, such as County Office of the Assessor. For example, the parcel data of Los Angeles County is from the Mapping & GIS Services Section, LA County Office of the Assessor; valid data vendors, including Regrid and ReportAll USA. They source their data from counties, states, municipalities and the designated vendors. Therefore, the data quality is highly reliable. Particularly, the data they provided is cleaned and standardized, facilitating its use.

This study covers sixteen counties, nearly half of all the thirty three counties that at least have some areas in LRA are designated as VHFHSZ. These sixteen counties contain around 7.1 million parcels, representing about 71 percent of all parcels in all designated counties. Figure 2 shows those counties.[14]

4.4 Road Network Data

The road network data in major California counties are collected from (Millard-Ball, 2022). Eleven counties in our sample are in the dataset.[15] I use this data to test the identification later. Figure A7 presents the street network in Los Angeles County.

4.5 Fire Perimeter Data

I collect the historical fire perimeter data from The Fire and Resource Assessment Program (FRAP) by CAL FIRE. FRAP records almost all fires that occurred on public and private lands in California, and considered as the most complete digital record of fire perimeters in California. This data is mainly used to measure wildfire risk, which is for calculating the correlation between wildfire risk and property value, as presented in Figure 1.

---

[14]The sixteen counties are: Contra Costa County, El Dorado County, Lake County, Los Angeles County, Monterey County, Nevada County, Orange County, Placer County, Riverside County, San Bernardino County, San Diego County, San Luis Obispo County, San Mateo County, Santa Barbara County, Santa Clara County, Shasta County, Sonoma County, Ventura County.

[15]The eleven counties are Los Angeles County, Ventura County, Sonoma County, Placer County, Riverside County, San Bernardino County, Monterey County, Orange County, Contra Costa County, and Santa Clara County.

5 Empirical Strategy

The main identification strategy in this paper is a spatial regression discontinuity design (SRDD). The VHFHSZ maps geographically split the areas into treated ones (inside VHFHSZ) and control ones (outside VHFHSZ). The SRDD is based on comparing areas that are barely inside to areas that are barely outside, i.e. around the VHFHSZ boundaries. This is a two-dimensional discontinuity with longitude and latitude in nature. Following Dell (2010) and Ambrus et al. (2020), I convert them to a one-dimensional running variable: the perpendicular distance from each 30×30m pixel to the closet point in the boundary. Figure A8 graphically shows how this distance is calculated.

The empirical specification:

$$Y_i = \delta D_i + f(Distance_i) + \mathbf{X}'_\mathbf{i}\beta + \phi_{c(i)} + \epsilon_i \tag{6}$$

where Y_i is the outcome of interest, including housing development, taxable property value during pre-2008 or 2008-2020 for pixel i. D_i is an indicator equals one if pixel i is inside the VHFHSZ, otherwise zero. δ is the coefficient of our interest, capturing the magnitude of discontinuity across the boundary. $Distance_i$ is the perpendicular distance from pixel i to the nearest VHFHSZ boundary. $f(Distance_i)$ is the RD polynomial function. $\mathbf{X}'_\mathbf{i}$ indicates the terrain characteristics at pixel level, including slope, roughness, and Terrain Ruggedness Index. Since there are no natural segments of the boundaries, I control the city fixed effects, $\phi_{c(i)}$, as a substitute for the segment fixed effects.[16] Pixels that are within 30 meters of boundary are dropped. Water pixels are also dropped since they are unsuitable for development. Figure A9 presents the density histograms of pixels at a 30-meter bin width.[17] Robust standard errors are clustered at local government level. Table 1 Panel [A] presents the summary statistics on key variables. On average, the housing development during post-map period areas in the full sample, which includes all LRA, is similar to the level observed in the boundary sample, which is restricted to 200 meters around the zone boundary. The taxable improved property value is higher in the boundary sample. On average, the boundary sample is with higher slope, roughness and Terrain Ruggedness Index. Table 1 Panel [B] presents the summary statistics on built year and taxable improved property value at parcel

---

[16]169 cities are in our final analysis sample. Additionally, for unincorporated areas in a county, I assign an unique city identifier to these pixels. We have sixteen such city identifiers, as the number of counties covered in this study. Thus, in total, we have 185 unique city identifiers.

[17]The reason to drop pixels with 30 meters of boundary is because it's very likely that there is measurement errors of the GIS data. This could be particularly an issue since local governments development permitting might also have some measurement error compared to the "true" boundary.

level conditional on the parcel was developed during post-map period. The mean built year is similar for the full sample and boundary sample, with 2015 and 2014 respectively. The taxable improved property value is slightly higher in the boundary sample than in the full sample.

This identification strategy faces one particular challenge, which is that the wildfire severity zone designation could be endogenous and correlated with other unobserved factors, such as amenities, infrastructures, and terrain characteristics. First, this endogeneity is practically less likely given the process and fuel models used in determining the zones, as detailed in Appendix C. Second, I take several identification tests: 1) pre-2008 results. I find no discontinuity across the zone boundary for housing development before 2008. Table A1 present the RD regression results. 2) By utilizing the road data in major counties in California, I find only 10.16% of the boundary are within 50 meters of the roads. Furthermore, the distribution is generally uniform across the distance. Figure A10 presents the density of distance from the VHFHSZ boundaries to the nearest main road. 3) I find no significant discontinuity across the zone boundary for slope, Terrain Ruggedness Index, roughness, and tree cover. Table A2 presents the RD regression results. All of the tests suggest that the zone boundaries are likely exogenous enough for SRDD identification use.

6 Results

6.1 The Effects on Housing Development

Figure 3 (a) presents the RD plot for housing development. We can observe a significant drop around the zone boundary. Table 2 presents the RD regression results based on equation (1). Housing development is defined at each pixel, as one if developed during 2008-2020, otherwise zero. The coefficient merely changes when terrain characteristics and city fixed effects are controlled. The estimate suggests that when being barely within very high wildfire severity zone, the probability for each pixel being developed reduces 0.006. This is 22.2% of the mean level of development, and equal to a 12 houses reduction for an area of 1.8 square kilometers. Table 5 extrapolates the effects when the boundary estimates expand to more areas into the regulated zones.[18] It's estimated that around thirteen thousands of houses

---

[18]The extrapolation should be interpreted with caution. The assumption is that the areas within VHFHSZ are the same as the areas near the boundary. It's likely that the more inside the zone, the suitability for the land to be developed decreases, e.g. it could be high mountains in the middle of the zone, which is very unlikely to be developed.

are less developed within 1 km distance inside the zone boundary. The numbers are larger when extrapolated to more inside areas. At the extreme, since there are 3494.62 square kilometers VHFHSZ in LRA in California.[19] Therefore, based on our estimate, because of the regulation, 23,297 houses are less built.

6.2 The Effects on Taxable Property Value

Figure 3 (b) presents the RD plot for taxable property value.[20] The estimates follow a similar pattern with the ones on housing development. Table 3 presents the RD regression results, which suggest that when barely within the zone, the taxable property value decreases 9.3%, which is 32.0% of the mean value. This is nontrivial. Table 5 extrapolates the estimates to areas at different distances inside the zone boundary. It's estimated that around 1.03 billion taxable property value is lost within 1 km distance inside the zone boundary, because of the regulation. The average property tax rate is 1.5%, then it indicates a 15.42 million dollars property tax revenue reduction. If go to extreme, extrapolating the estimate to all VHFHSZ areas, this reduction equals to around 1.7 billion dollars reduction in property value and a 26 million dollars property tax revenue.

6.3 Robustness Check

Following the thoughts from Ganong and Jäger (2018), I perform a permutation test moving the boundary inside the true one at an interval of 30 meters starting from 60 meters till 180 meters.[21] If the true treatment effect is significant, then it should be much larger in absolute value than this full set of placebo estimates. Table A4 presents the results. Almost all of the estimates in the table are statistically insignificant, and the magnitude is much smaller compared to the true ones.[22] The results support that the boundary RD estimates are likely the true treatment effects of interest.

---

[19]This is about 29 times of the area of San Francisco County.

[20]In our main results, I use log(taxable property value) for analysis. Our results are robust when using the level values of taxable property value. Table A3 presents the main estimates using level values. The results on pre-period, heterogeneous effects and permutation test are all robust when using level values. For the sake of brevity, the tables are not shown in the paper, and available upon request.

[21]As discussed in Section 5, I drop pixels that are within 30 meters of boundary to avoid measurement error. Therefore, I start from moving outside 60 meters, rather than 30 meters.

[22]The 150m scenario has a statistically significant estimate on housing development. However, the magnitude is still much smaller than the true one and is a positive one.

6.4 Heterogeneous Effects with Local Property Tax Revenue Dependency

The incentive to increase property tax revenue should be stronger for local jurisdictions with higher dependency on property tax revenue. To test this, I collected the Census Bureau's Census of Governments and Annual Survey of State and Local Government Finances for data on individual county and municipal/township governments. To avoid endogeneity issues, I used data from 2007, one to four years prior to the release of the recommended map. The census surveys the complete count of governments every five years, and fortunately, 2007 is one of those years. Specifically, I used the Government Finance Database (Pierson et al., 2015), which is an effort to provide a single, coherent common database for empirical analysis on local finance. I define a dummy at the city/county level based on whether the dependency on property tax revenue for a local government is above or below the median dependency of all local governments in California, equals one if above. Data appendix B.3 provides the details on the data match and cleaning.

I perform the same RD regression analysis for the two subsamples. Table 4 panel A presents the results using the above median sample. The magnitude on development is -0.009 and statistically significant at 5% level, much larger than the overall estimate in absolute value. The mean is 0.030, thus this indicates a nearly 30% decrease of mean. The magnitude on taxable property value is also much higher than the overall estimate, particularly, the mean in this subsample is slightly lower. Thus the reduction of taxable property value is equal to about 50% of the mean, which is much higher than the average 32%. Table 4 panel B presents the results using the below median sample. There are two notes deserving attention. First, the magnitude is significantly smaller than the ones in above median sample. Second, almost all of them are statistically insignificant. The patterns suggest that the main results are likely to be driven by the local governments that have higher financial dependency on property tax revenue.

7 Conclusion

Climate risk and its cost on society is accelerating. However, at the same time, evidence suggests massive ineffective adaptation to the risk: huge number of people, housing and economic activities remain in high climate risk areas, such as coastal regions vulnerable to sea level rise, areas prone to wildfires, and regions susceptible to flooding. The inefficiency comes from multiple dimensions of private market failures. This paper examines the effects of

state-level building codes on housing development in wildfire-prone areas of California using a spatial regression discontinuity design around the regulatory map boundaries. I combine high resolution data at 30×30m pixel level with millions of parcels in sixteen counties in California. The results indicate that there is a significant decrease in the number of houses developed and taxable property value in the regulated values.

Given that the local governments are practically responsible for putting building codes and permitting constructions, why the state regulation is necessary and has such large reduction effects? I propose that the local governments face a trade-off between restricting housing development in climate risky areas, thereby reducing risk exposure and the potential damage from climate disasters, and capturing more property tax revenue generated in these climate risky areas. The local governments essentially have a pervasive incentive to allow for over-development in areas with high climate risk given the disproportionate property tax revenue through the permitting. This leads them to ineffectively correct the private market failures. However, central governments, which have no such incentive, can intervene and correct this specific market failure, restoring efficiency. By combining the house data with local public finance census data, I find that reductions are greater in local jurisdictions more dependent on property tax revenue, aligning with the predictions from the theoretical model I propose.

This analysis enhances our understanding of the importance of incentives across different levels of governments. Particularly, local governments, as fundamental forces in combating climate risk and facilitating climate adaptation, face more challenges. This paper emphasizes this by theoretically proposing the property tax revenue incentive for local governments, and empirically testing it. The results generally shed light on the challenges of climate adaptation (e.g. managed retreat) where property tax incentives may create inefficient local government policies to correct housing market failures.

References

J. Alm, R. D. Buschman, and D. L. Sjoquist. Foreclosures and local government revenues from the property tax: The case of georgia school districts. *Regional Science and Urban Economics*, 46:1–11, 2014.

A. Ambrus, E. Field, and R. Gonzalez. Loss in the time of cholera: Long-run impact of a disease epidemic on the urban landscape. *American Economic Review*, 110(2):475–525, 2020.

J. Anders and R. Campbell. The "gorilla in the closet": Regulatory enforcement under federalism. 2024.

C. Balboni. In harm's way? infrastructure investments and the persistence of coastal cities. *American Economic Review*, 115(1):77–116, 2025.

J. L. Barnett, C. L. Sheckells, S. Peterson, and E. M. Tydings. 2012 census of governments: Financeâstate and local government summary report. *Economy-Wide Statistics Briefs: Public Sector. G12-CG-ALFIN. US Department of Commerce, Economics and Statistics Administration, US BUREAU OF THE CENSUS. December*, 17:12, 2014.

P. Baylis and J. Boomhower. The economic incidence of wildfire suppression in the united states. *American Economic Journal: Applied Economics*, 15(1):442–473, 2023.

P. W. Baylis and J. Boomhower. Mandated vs. voluntary adaptation to natural disasters: the case of us wildfires. Technical report, National Bureau of Economic Research, 2022.

J. K. Brueckner and H.-A. Kim. Urban sprawl and the property tax. *International Tax and Public Finance*, 10:5–23, 2003.

M. Burchfield, H. G. Overman, D. Puga, and M. A. Turner. Causes of sprawl: A portrait from space. *The Quarterly Journal of Economics*, 121(2):587–633, 2006.

California State Board of Equalization. California state board of equalization: 2016-2017 annual report, 2018. URL https://www.boe.ca.gov/aboutBOE/annual/2016-17/pub306.pdf.

S. Calonico, M. D. Cattaneo, and R. Titiunik. Robust nonparametric confidence intervals for regression-discontinuity designs. *Econometrica*, 82(6):2295–2326, 2014.

Congressional Research Service. Wildfire statistics, 2023. URL https://crsreports.congress.gov/product/pdf/IF/IF10244.

M. Coronese, F. Lamperti, K. Keller, F. Chiaromonte, and A. Roventini. Evidence for sharp increase in the economic damages of extreme natural disasters. *Proceedings of the National Academy of Sciences*, 116(43):21450–21455, 2019.

M. Dell. The persistent effects of peru's mining mita. *Econometrica*, 78(6):1863–1903, 2010.

First Street Foundation. The 9th national risk assessment: The insurance issue, 2023. URL https://report.firststreet.org/9th-National-Risk-Assessment-The-Insurance-Issue.pdf.

P. Ganong and S. Jäger. A permutation test for the regression kink design. *Journal of the American Statistical Association*, 113(522):494–504, 2018.

C. Garnache. Does the salience of climate-related risk affect asset prices? *Available at SSRN 3398404*, 2023.

E. L. Glaeser and B. A. Ward. The causes and consequences of land use regulation: Evidence from greater boston. *Journal of urban Economics*, 65(3):265–278, 2009.

M. Gonzalez-Navarro and C. Quintana-Domeque. Paving streets for the poor: Experimental analysis of infrastructure effects. *Review of Economics and Statistics*, 98(2):254–267, 2016.

J. Gyourko and S. McCulloch. Minimum lot size restrictions: Impacts on urban form and house price at the border. Technical report, National Bureau of Economic Research, 2023.

B. H. Harris, B. D. Moore, and U.-B. T. P. Center. Residential property taxes in the united states. *Urban-Brookings Tax Policy Center Working Paper*, 2, 2013.

M. Hino and M. Burke. The effect of information about climate risk on property values. *Proceedings of the National Academy of Sciences*, 118(17):e2003374118, 2021.

A. Hsiao. Sea level rise and urban adaptation in jakarta. *Technical Report*, 2023.

J. Jung and M. D. Makowsky. The determinants of federal and state enforcement of workplace safety regulations: Osha inspections 1990–2010. *Journal of regulatory economics*, 45:1–33, 2014.

Katz and Marr. America is increasingly building homes in disaster-prone areas, 2022. URL https://www.redfin.com/news/homes-built-disaster-prone-areas/. https://www.redfin.com/news/homes-built-disaster-prone-areas/. Accessed January 10, 2025.

B. Knight. Endogenous federal grants and crowd-out of state government spending: Theory and evidence from the federal highway aid program. *American Economic Review*, 92(1):71–92, 2002.

X. Li, S. Gopalakrishnan, and H. A. Klaiber. Local adaptation and unintended coastal vulnerability: the effect of beach nourishment on residential development in north carolina. *Journal of the Association of Environmental and Resource Economists*, 11(3):523–548, 2024.

C. S. Lim and A. Yurukoglu. Dynamic natural monopoly regulation: Time inconsistency, moral hazard, and political environments. *Journal of Political Economy*, 126(1):263–312, 2018.

Y. Lin, T. K. McDermott, and G. Michaels. Cities and the sea level. *Journal of Urban Economics*, 143:103685, 2024.

Lincoln Institute of Land Policy and Minnesota Center for Fiscal Excellence. 50-state property tax comparison study, 2023. URL https://www.lincolninst.edu/publications/other/50-state-property-tax-comparison-study-2022. https://www.lincolninst.edu/publications/other/50-state-property-tax-comparison-study-2022/. Accessed August 20, 2024.

B. Lutz. Quasi-experimental evidence on the connection between property taxes and residential capital investment. *American Economic Journal: Economic Policy*, 7(1):300–330, 2015.

L. Ma, M. Walls, M. Wibbenmeyer, and C. Lennon. Risk disclosure and home prices: evidence from california wildfire hazard zones. *Land Economics*, 100(1):6–21, 2024.

M. L. Mann, P. Berck, M. A. Moritz, E. Batllori, J. G. Baldwin, C. K. Gately, and D. R. Cameron. Modeling residential development in california from 2000 to 2050: Integrating wildfire risk, wildland and agricultural encroachment. *Land use policy*, 41:438–452, 2014.

C. J. Mayer and C. T. Somerville. Land use regulation and new construction. *Regional Science and Urban Economics*, 30(6):639–662, 2000.

S. J. McCoy and R. P. Walsh. Wildfire risk, salience & housing demand. *Journal of Environmental Economics and Management*, 91:203–228, 2018.

S. Meier, R. J. Elliott, and E. Strobl. The regional economic impact of wildfires: Evidence from southern europe. *Journal of Environmental Economics and Management*, 118:102787, 2023.

A. Millard-Ball. The width and value of residential streets. *Journal of the American Planning Association*, 88(1):30–43, 2022.

R. K. Miller, C. B. Field, and K. J. Mach. Factors influencing adoption and rejection of fire hazard severity zone maps in california. *International Journal of Disaster Risk Reduction*, 50:101686, 2020.

National Interagency Fire Center. Total wildland fires and acres (1983-2022), 2022. URL https://www.nifc.gov/fire-information/statistics/wildfires. https://www.nifc.gov/fire-information/statistics/wildfires. Accessed July 26, 2024.

NOAA National Centers for Environmental Information. 2023: A historic year of u.s. billion-dollar weather and climate disasters, 2024a. URL https://www.climate.gov/news-features/blogs/beyond-data/2023-historic-year-us-billion-dollar-weather-and-climate-disasters. Accessed Sep 1, 2024.

NOAA National Centers for Environmental Information. U.s. billion-dollar weather and climate disasters (2024), 2024b. URL https://www.ncei.noaa.gov/access/billions/. https://www.ncei.noaa.gov/access/billions/. Accessed July 26, 2024.

A. Ostriker and A. Russo. The effects of floodplain regulation on housing markets. *URL https://ostriker. github. io/papers/Ostriker-Russo floodplain-regulations. pdf*, 2024.

K. Pierson, M. L. Hand, and F. Thompson. The government finance database: A common resource for quantitative research in public financial analysis. *PloS one*, 10(6):e0130119, 2015.

Q. Ren and J. West. Cleaner waters and urbanization. *Journal of Environmental Economics and Management*, 122:102874, 2023a.

Q. Ren and J. West. Who benefits from surface water pollution programs? *Working paper*, 2023b.

A. Saiz. The geographic determinants of housing supply. *The Quarterly Journal of Economics*, 125(3):1253–1296, 2010.

A. P. Shafran. Risk externalities and the problem of wildfire risk. *Journal of Urban Economics*, 64(2):488–495, 2008.

L. Shi and A. M. Varuzzo. Surging seas, rising fiscal stress: Exploring municipal fiscal vulnerability to climate change. *Cities*, 100:102658, 2020.

J. Song. The effects of residential zoning in us housing markets. *Available at SSRN 3996483*, 2021.

Y. Song and Y. Zenou. Property tax and urban sprawl: Theory and implications for us cities. *Journal of urban economics*, 60(3):519–534, 2006.

K. R. Wagner. Adaptation and adverse selection in markets for natural disaster insurance. *American Economic Journal: Economic Policy*, 14(3):380–421, 2022.

R. W. Wassmer. Further empirical evidence on residential property taxation and the occurrence of urban sprawl. *Regional Science and Urban Economics*, 61:73–85, 2016.

wildfirerisk.org. Updates to wildfire risk to communities reveal 115 million people living with high wildfire risk, 2024. URL https://headwaterseconomics.org/natural-hazards/updates-to-wildfire-risk-to-communities/. https://wildfirerisk.org/. Accessed July 26, 2024.

World Economic Forum. The global risks report 2024, 2024.

Figures and tables

Figure 1: Correlation between wildfire risk and taxable improved property value
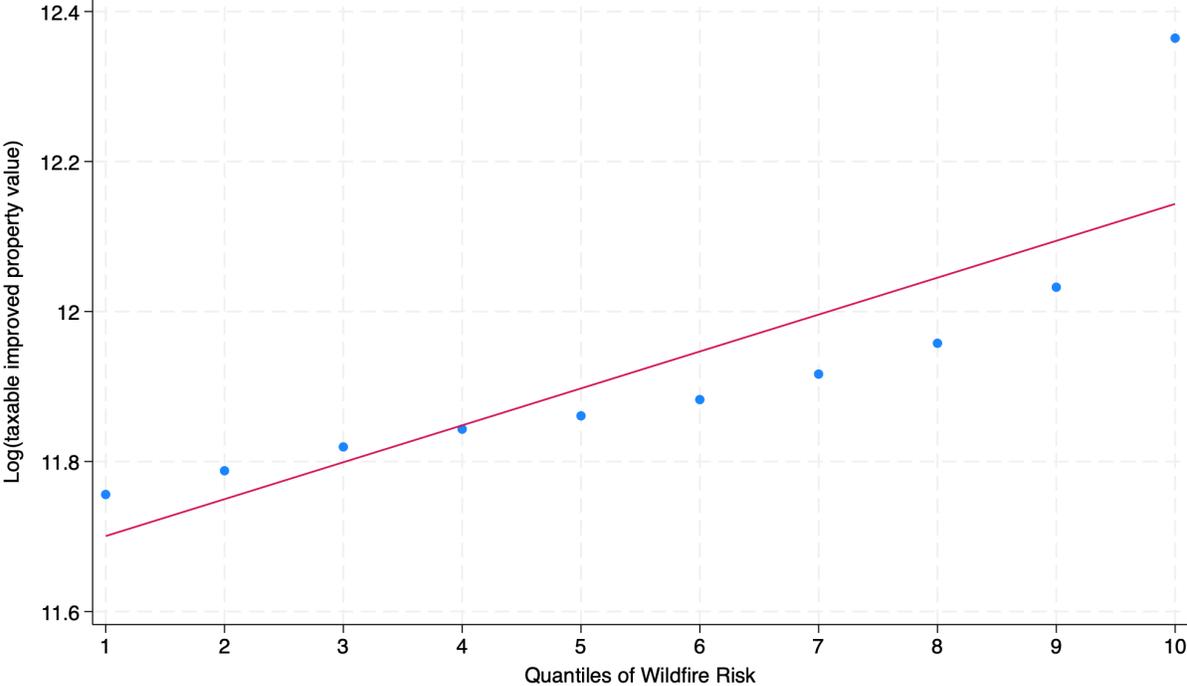

Notes: Wildfire risk is measured by the negative value of distance from each parcel to the fire perimeter. By this construction, the higher the value the higher wildfire risk the parcel is. Fire perimeter data is from The Fire and Resource Assessment Program (FRAP) by CAL FIRE. This figure uses the version of Firep23_1, which was released in May 2024, and restricts the fires to those that occurred in Los Angeles (LA) County. It records almost all historical fires (1878-2023) that occurred on public and private lands in LA. Distance is calculated from each parcel centroid to the nearest fire perimeter. For parcel centroids that are within fire burn area, the distance is assigned with zero. The points are based on over 2 million parcel observations in LA. Each point is the average of log(taxable improved property value) over the ten quantiles of wildfire risk, after controlling for construction year and building square footage. The red line is the linear fitted line along the points.

Figure 2: Counties with VHFHSZ in LRA and County Coverage in This Study
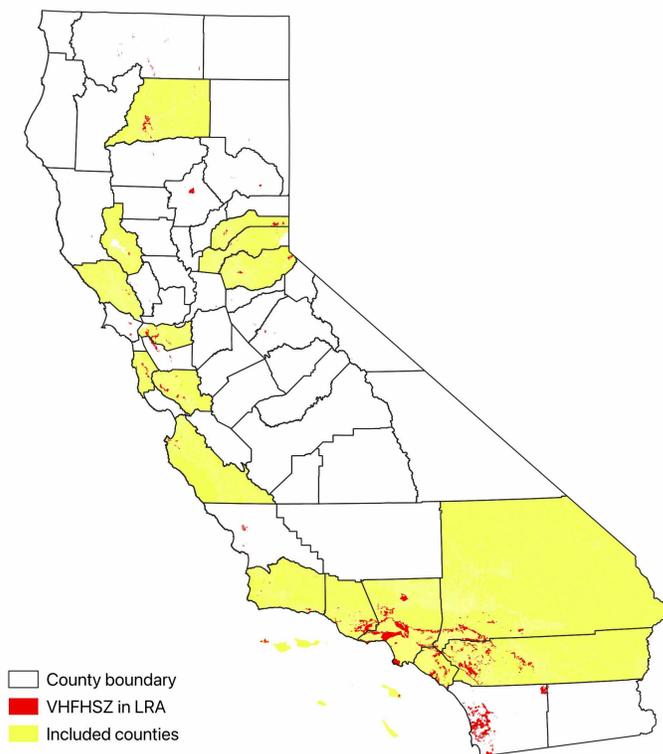
Notes: The figure presents counties with VHFHSZ in Local Responsibility Areas, and the sixteen counties that are covered by this study, representing around 71% of all parcels in all VHFHSZ-affected counties.

Figure 3: RD Plots for Housing Development and Taxable Improved Property Value
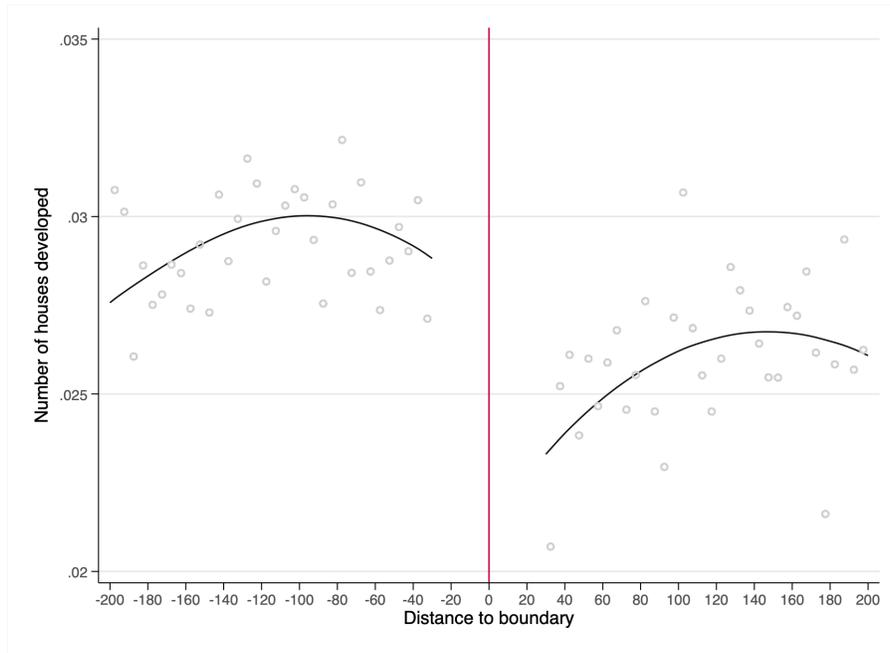
(a) Housing Development
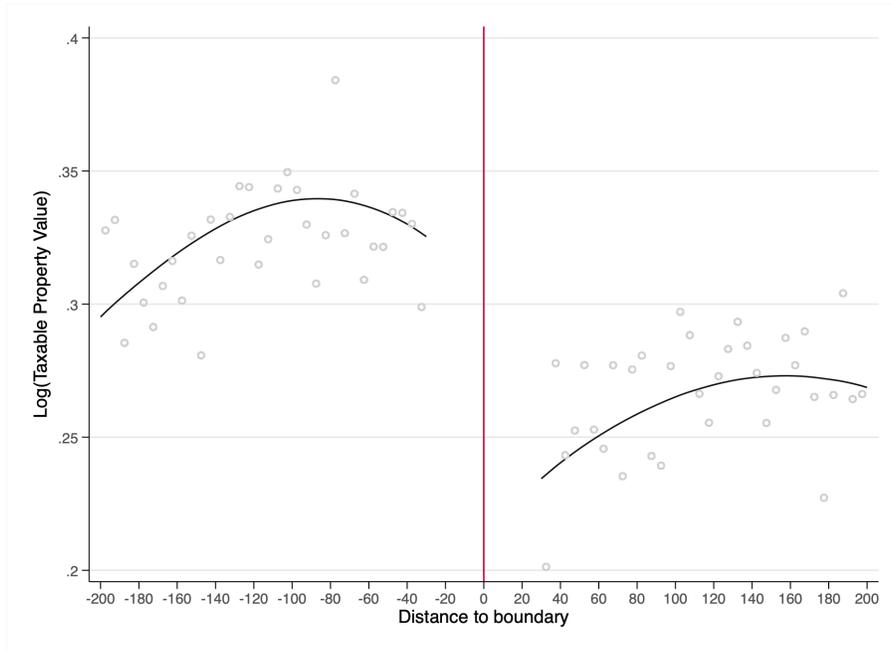
(b) Log(Taxable Improved Property Value)

Notes: Hollow circle points are 5-meter binned averages from predicted values using a regression controlling city fixed effects using observations at 30×30m pixel. Distance is measured in meters, with positive values being inside the VHFHSZ, and negative values being outside the VHFHSZ. The solid vertical red line represents the VHFHSZ boundary. Solid trend lines are the Kernel-weighted local polynomial smoothing with a triangular kernel and 200-meter bandwidth.

	Full sample (1)	Boundary sample (2)
Panel [A]: Pixel level		
Housing development	0.03	0.03
Taxable improved property value (in logs)	0.26	0.29
Slope	6.01	7.50
Roughness	10.79	13.43
Terrain Ruggedness Index	16.98	20.77
Panel [B]: Parcel level		
Year built	2015	2014
Taxable improved property value (in logs)	11.11	11.59

Notes: Each observation in Panel [A] is a 30×30m pixel. Each observation in Panel [B] is a developed parcel after the map release. Housing development is an indicator, equals one if a building developed during the year when the map was recommended-2020, otherwise zero. Taxable improved property values are missing in three counties: Contra Costa, Montery, Shasta, thus they are excluded in the sample. Slope is the angle of inclination of the terrain and is expressed in degrees. Roughness is computed from the elevation. It's the degree of irregularity of the surface. TRI summarizes the change in elevation within the 3×3 pixel grid, and is a measurement of terrain heterogeneity. All of three indexes are from the National Land Cover Database (NLCD) 2006, when is the pre-map period. Full sample includes all LRA areas. Boundary sample restricts to 200 meters around the boundary.

Table 2: Spatial Regression Discontinuity Estimates: housing development

	(1)	(2)	(3)
Inside VHFHSZ	-0.006*	-0.006**	-0.006**
	(0.003)	(0.003)	(0.003)
Terrain characteristics		Yes	Yes
City fixed effects			Yes
Dependent variable mean	0.027	0.027	0.027
Bandwidth (meters)	159	159	159
Observations	915,917	915,917	915,917

Notes: Each observation is a 30×30m pixel. Optimal bandwidth is calculated as in Calonico et al. (2014) and using a triangular weighting kernel. Housing development is an indicator, equals one if a building developed during the year when the map was recommended-2020, otherwise zero. Terrain characteristics include slope, roughness, and Terrain Ruggedness Index. Standard errors are clustered at city level.

*** p<0.01, ** p<0.05, * p<0.1

Table 3: Spatial Regression Discontinuity Estimates: log(taxable improved property value)

	(1)	(2)	(3)
Inside VHFHSZ	-0.104***	-0.109***	-0.093***
	(0.034)	(0.034)	(0.030)
Terrain characteristics		Yes	Yes
City fixed effects			Yes
Dependent variable mean	0.291	0.291	0.291
Bandwidth (meters)	152	152	152
Observations	782,026	782,026	782,026

Notes: Each observation is a 30×30m pixel. Optimal bandwidth is calculated as in Calonico et al. (2014) and using a triangular weighting kernel. Taxable improved property values are missing in three counties: Contra Costa, Montery, Shasta, thus they are excluded in the sample. Standard errors are clustered at city level.

*** p<0.01, ** p<0.05, * p<0.1

Table 4: Heterogeneous Effects with Local Property Tax Revenue Dependency

	Housing development			Log(taxable improved property value)		
	(1)	(2)	(3)	(4)	(5)	(6)
Panel [A]: Above Median Sample						
Inside VHFHSZ	-0.010**	-0.010**	-0.009**	-0.141***	-0.145***	-0.127***
	(0.005)	(0.005)	(0.004)	(0.053)	(0.053)	(0.041)
Terrain characteristics		Yes	Yes		Yes	Yes
City fixed effects			Yes			Yes
Dependent variable mean	0.025	0.025	0.025	0.257	0.257	0.257
Bandwidth (meters)	153	153	153	134	134	134
Observations	439,337	439,337	439,337	331,092	331,092	331,092
Panel [B]: Below Median Sample						
Inside VHFHSZ	-0.001	-0.002	-0.002	-0.067	-0.072*	-0.060
	(0.003)	(0.003)	(0.003)	(0.041)	(0.040)	(0.038)
Terrain characteristics		Yes	Yes		Yes	Yes
City fixed effects			Yes			Yes
Dependent variable mean	0.030	0.030	0.030	0.323	0.323	0.323
Bandwidth (meters)	154	154	154	172	172	172
Observations	436,971	436,971	436,971	460,569	460,569	460,569

Notes: Each observation is a 30×30m pixel. Optimal bandwidth is calculated as in Calonico et al. (2014) and using a triangular weighting kernel. Housing development is an indicator, equals one if a building in a parcel was developed during 2008-2020 and overlapped with the pixel, otherwise zero. Terrain characteristics include slope, roughness, and Terrain Ruggedness Index. Taxable improved property values are missing in three counties: Contra Costa, Montery, Shasta, thus they are excluded in the sample used in columns (4)-(6). Above Median Sample is the subsample of pixels within local jurisdictions where the dependency on property tax revenue is above the median value in all counties and cities in California, otherwise it belongs to the Below Median Sample. Standard errors are clustered at city level.

*** p<0.01, ** p<0.05, * p<0.1

Table 5: Extrapolation Scenarios

	1 km	2 km	All
Number of pixels	2,140,583	2,632,517	2,862,260
Number of houses	-12,843	-15,795	-17,174
Log(taxable improved property value)	-9.3%	-9.3%	-9.3%
Average improved taxable property value (per pixel) ($)	5164.86	5018.69	4796.78
Taxable property value (billion $)	-1.03	-1.23	-1.28
NPV of taxable property value (billion $)	-51.50	-61.50	-64.00
Property tax revenue (million $)	-15.42	-18.43	-19.15

Notes: This table presents the total number of houses, taxable improved property value and property tax revenue that would be reduced if the boundary estimate is extrapolated to more inside areas within VHFHSZ. Three scenarios are considered based on the distance from the boundary to VHFHSZ areas. This extrapolation is for our analysis sample data. If extrapolated to all VHFHSZ in LRA in California, which includes counties that are not included in the analysis (e.g. San Diego County), the number of houses that would be reduced is 23,297, the taxable improved property value reduction is 1.7 billion dollars, and the property tax revenue reduction is around 26 million dollars. Property tax revenue is calculated using the average tax rate 1.5%. NPV is the net present value caculated at a discount rate of 2%, which is the constraint rate set by Proposition 13 in California.

A   Appendix figures and tables

Figure A1: Trends on Acres Burned: 1987-2020
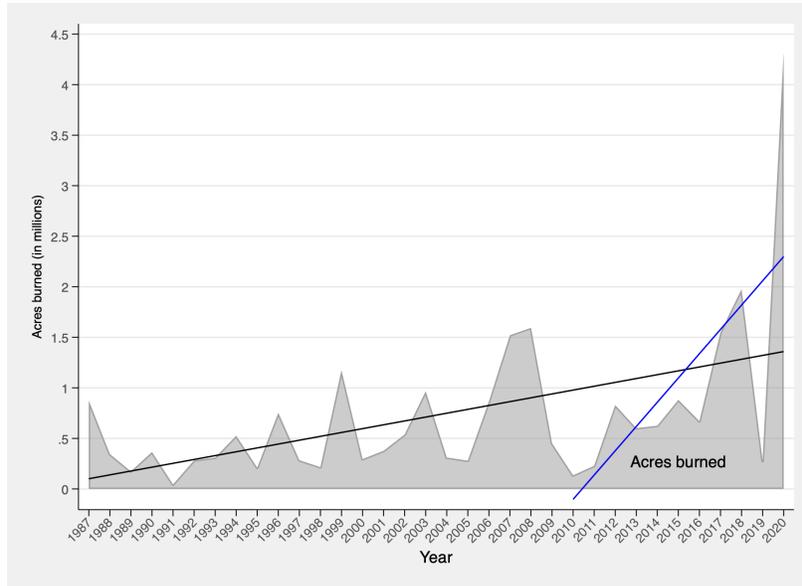
(a) California Trend on Acres Burned: 1987-2020
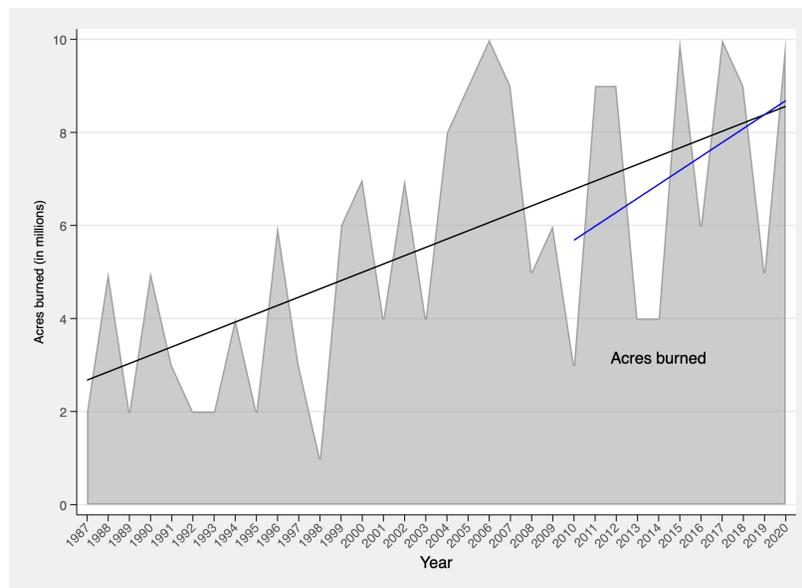
(b) US National Trend on Acres Burned: 1987-2020

Notes: The Acres burned data is from National Interagency Fire Center. The black line is the linear fitted trend for 1987-2020. The blue line presents the linear fitted trend for 2010-2020. The slope is much higher in the recent decade, which suggests a strongly increasing trend.

Figure A2: VHFHSZ Maps in Local Responsibility Areas

Legend
- LRA
- VHFHSZ in LRA
- County boundary
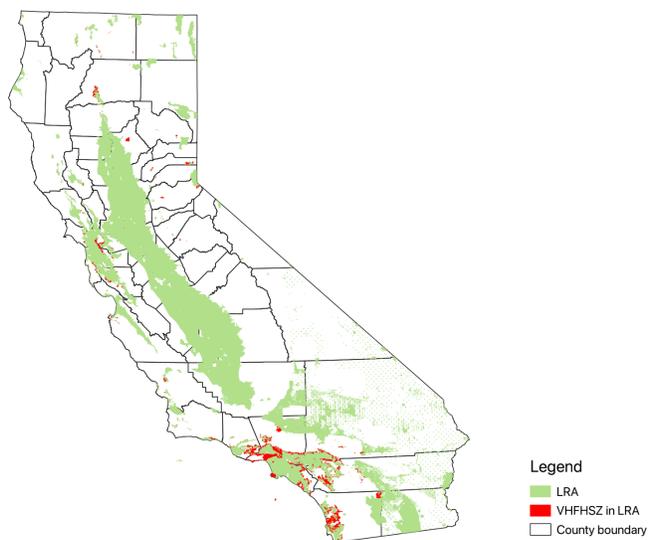
(a) Local Responsibility Areas and VHFHSZ
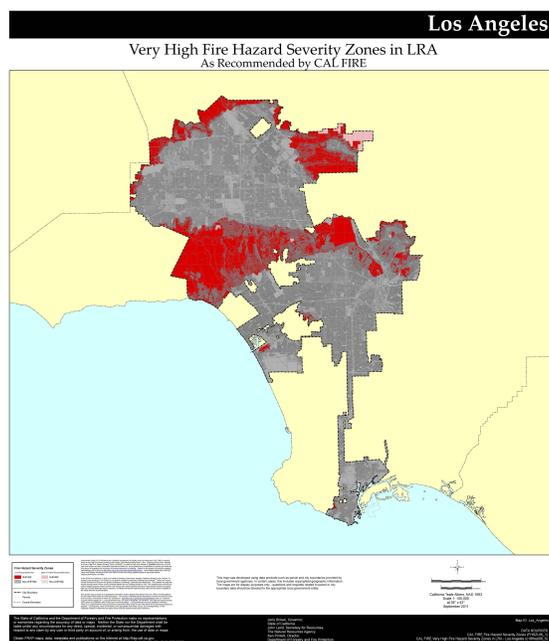
(b) VHFHSZ Map in Los Angeles City

Notes: Figure (a) presents all Local Responsibility Areas (LRA) and VHFHSZ in California. Figure (b) presents an example of the VHFHSZ map in Los Angeles City. Data are collected from CAL FIRE.

A2

Figure A3: Tax Revenue Trends in California
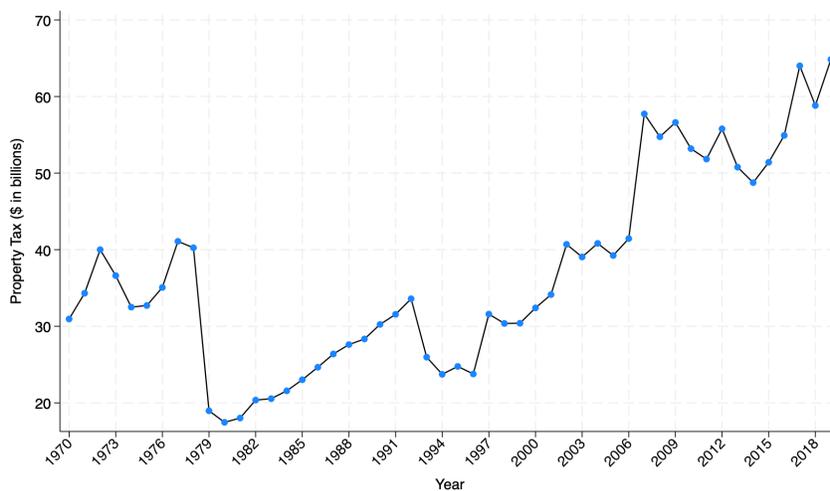
(a) Property Tax Revenue in California Local Governments: 1970-2019
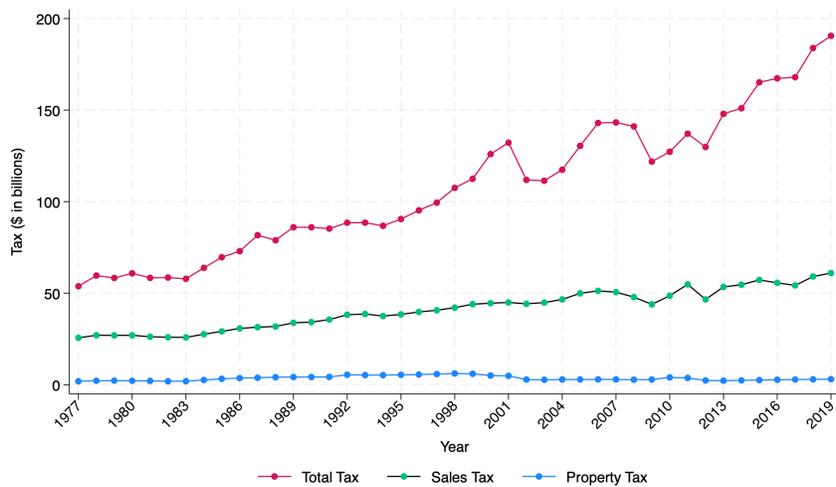
(b) State-collected Taxes in California: 1977-2019

Notes: Property tax data are from the Government Finance Database (Pierson et al., 2015). The values are in 2020 dollars. State-collected taxes start from 1977 since this is the earliest time that consistent data is available.

Figure A4: Climate Risk, Externality and Private Market Failures
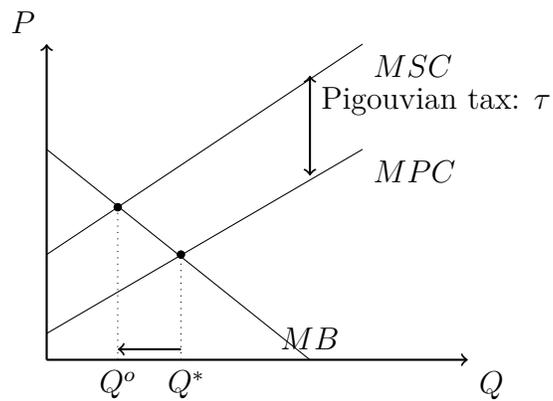
Notes: This figure presents the market failures in housing development, and how they can be corrected via a Pigouvian tax by the government.

Figure A5: The Relative Rankings of Housing Development Quantities

Q

Private Market Failures Q^*

High Dependency Q^*_{gH}

Overall Q^*_g

Low Dependency Q^*_{gL}

Efficiency Q^o
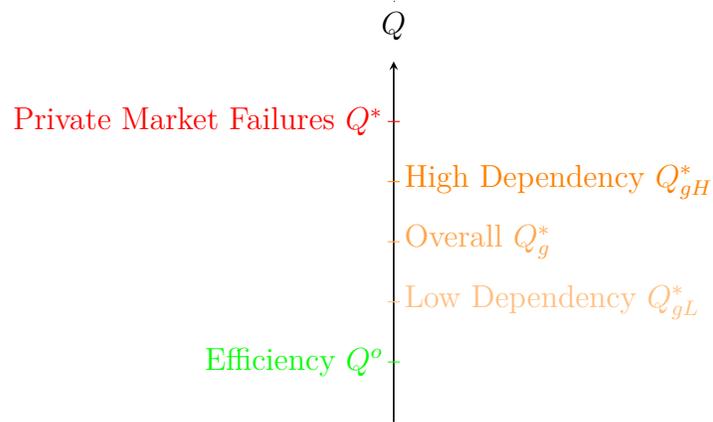
Notes: This figure presents the relative rankings of the housing development quantities at different scenarios. Private market failures secnario indicates the quantity without any regulation and with no property tax revenue incentive. High dependency indicates the scenario that the local government is highly dependent on property tax revenue as a revenue source. Low dependency indicates the scenario that the local government is less dependent on property tax revenue as a revenue source. Overall indicates the scenario at an average dependency. Efficiency indicates all private market failures are corrected and there is no property tax revenue incentive.

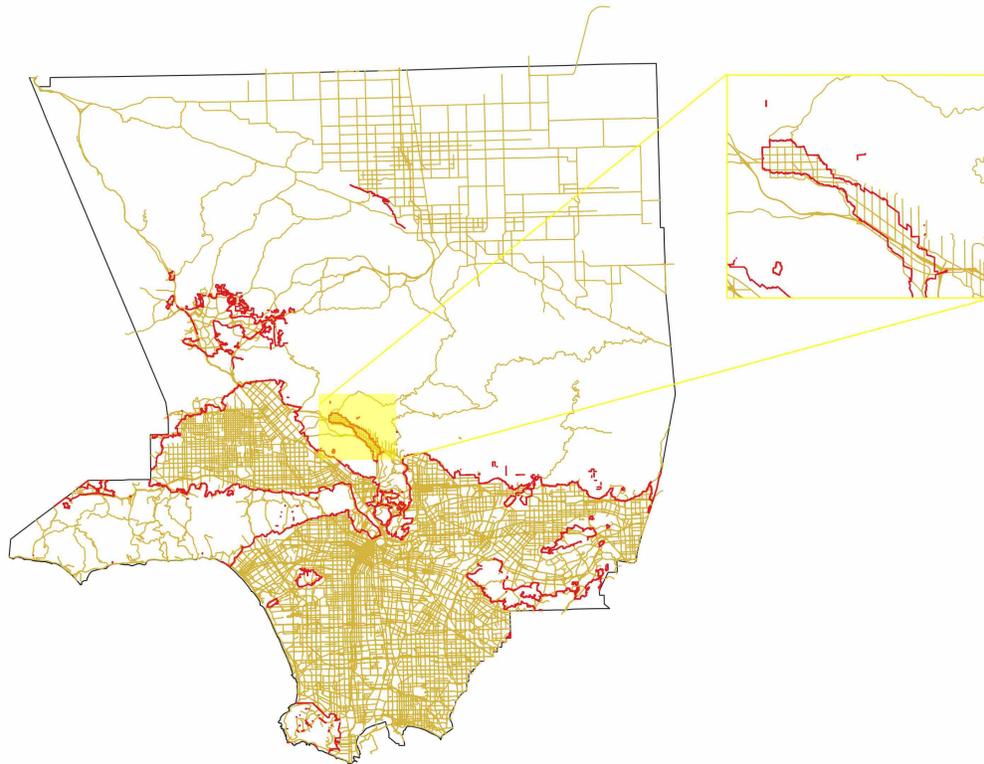Figure A6: Land Cover at 30×30m pixels
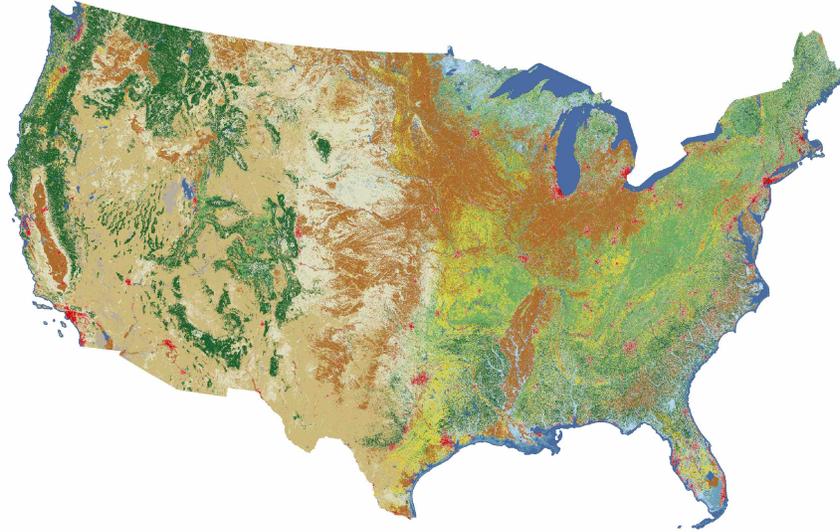

(a) Contiguous US
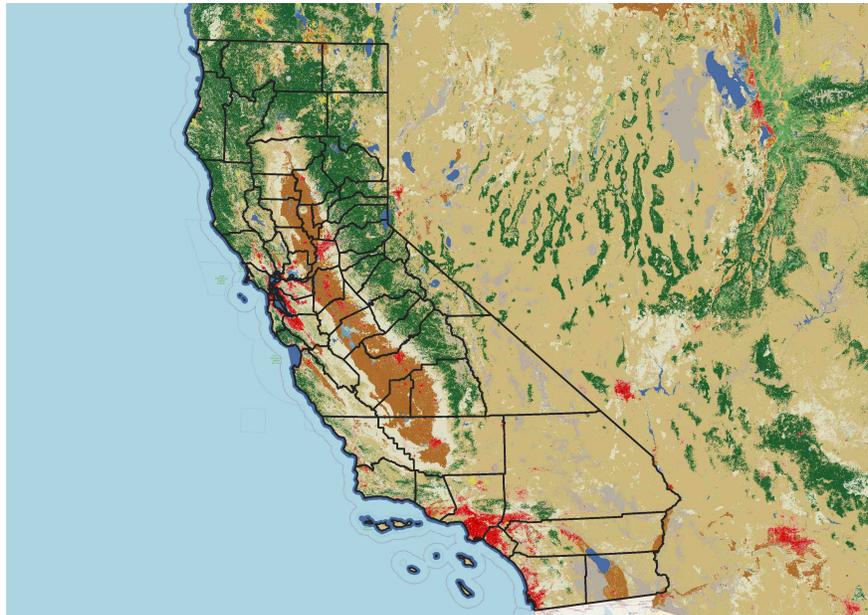
(b) California

Notes: The maps capture a 2006 snapshot. Data sources from National Land Cover Database 2006. Black lines are county boundaries. There are around 471 million 30×30m pixels in California.

Figure A7: Road Network in Los Angeles County

Notes: Data comes from Millard-Ball (2022). Yellow lines are roads. Red lines are VHFHSZ boundaries.

Figure A8: Perpendicular distance from each 30×30m pixel to the nearest VHFHSZ boundary
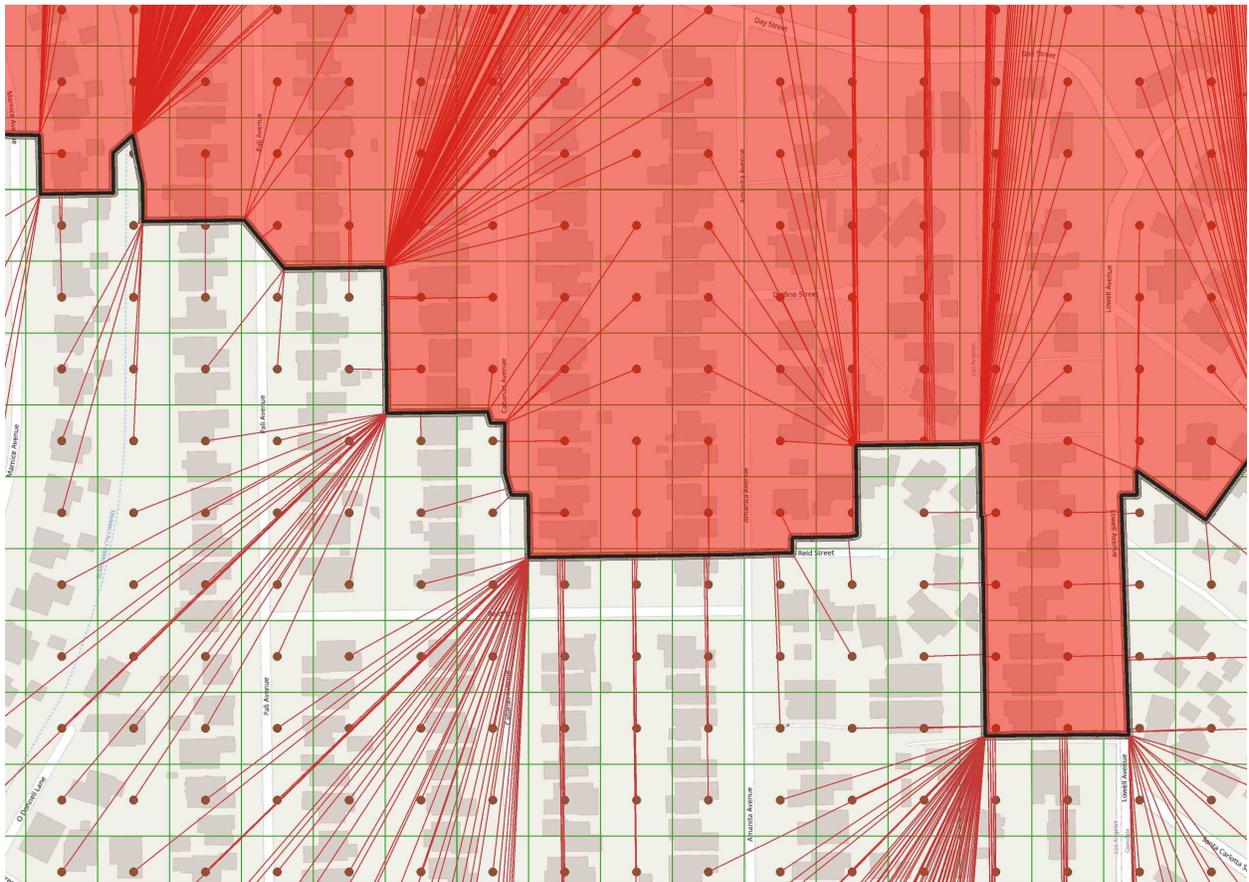
Notes: Each solid point is the centroid of the pixel. Green squares are 30×30m pixels. The black lines are the VHFHSZ boundaries, where red-shaded areas are the VHFHSZ. The red straight lines are the distances from the pixel centroids to the nearest point on the boundary.

Figure A9: Density of Pixels Across Distance-to-boundary Bins
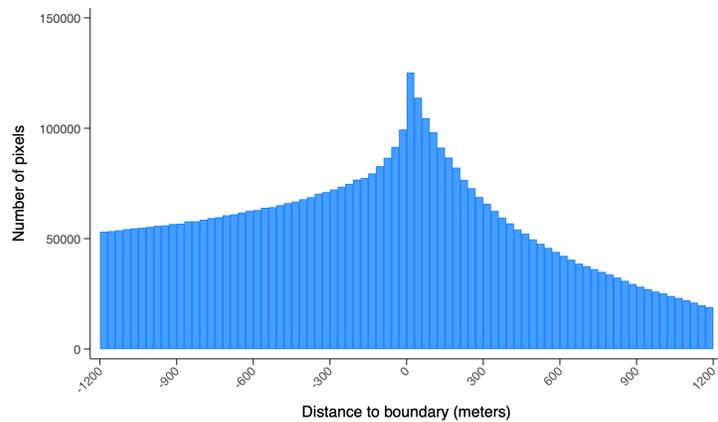
(a) All pixels
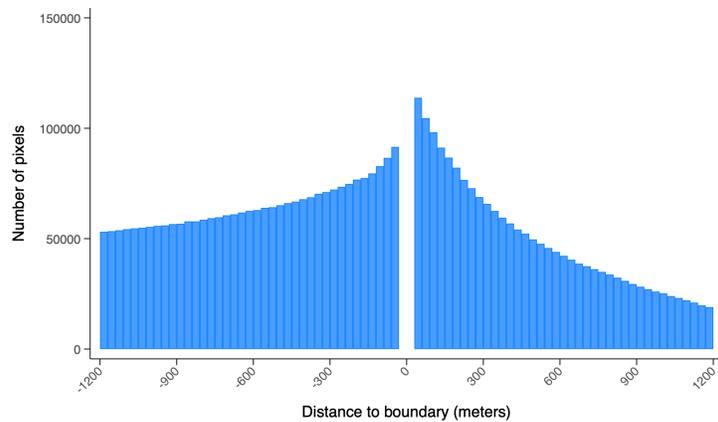
(b) Dropping pixels within 30 meters of boundary

Notes: Each bin has a width of 30 meters. Distance is measured in meters, with positive values being inside the VHFHSZ, and negative values being outside the VHFHSZ.

Figure A10: Density of Distance from Boundary to Roads

kernel = epanechnikov, bandwidth = 2.9962
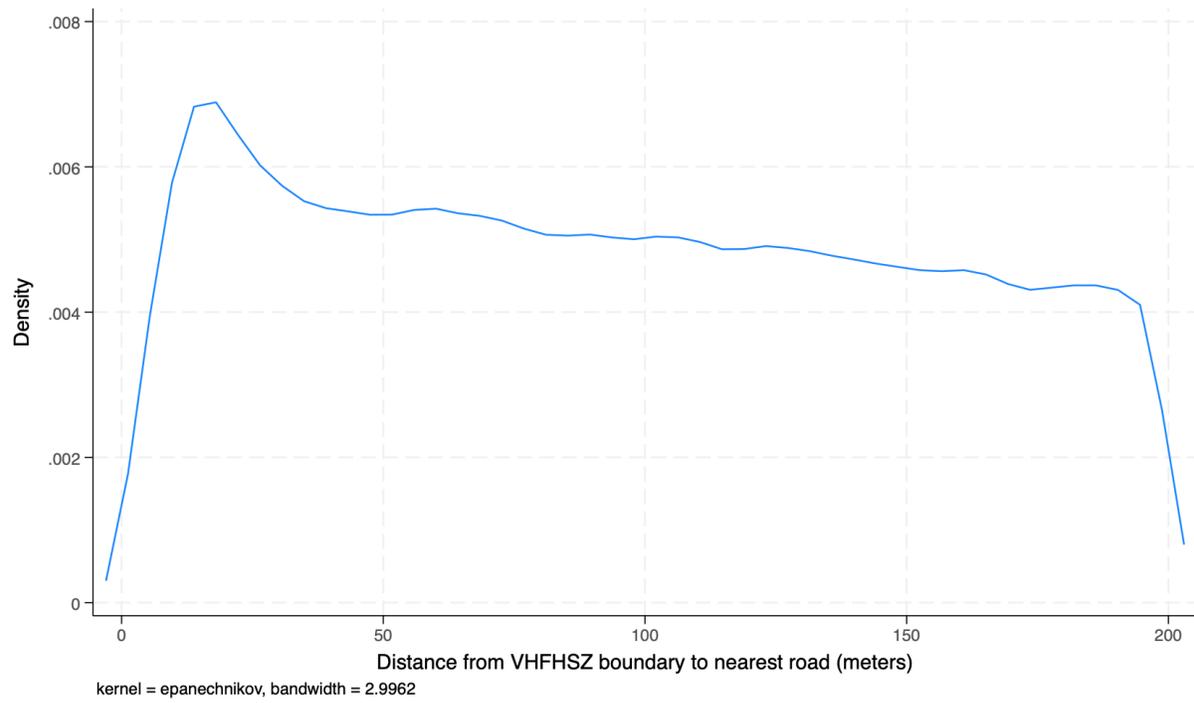
Notes: This figures presents the density of distance from the VHFHSZ boundaries to the nearest main road. Road network data fro ten counties are available and included: Los Angeles County, Ventura County, Sonoma County, Placer County, Riverside County, San Bernardino County, Monterey County, Orange County, ContraCosta County, Santa Clara County. Only 10.16% of the boundary are within 50 meters of the roads.

Table A1: Placebo Test: pre-period

	Housing development			Log(taxable improved property value)		
	(1)	(2)	(3)	(4)	(5)	(6)
Inside VHFHSZ	0.011	0.012	0.010	0.163	0.172	0.146
	(0.011)	(0.011)	(0.011)	(0.136)	(0.136)	(0.137)
Terrain characteristics		Yes	Yes		Yes	Yes
City fixed effects		Yes			Yes	
Dependent variable mean	0.154	0.154	0.154	1.733	1.733	1.733
Bandwidth (meters)	184	184	184	183	183	183
Observations	1,068,322	1,068,322	1,068,322	957,709	957,709	957,709

Notes: This table presents RD regression results of housing development during pre map period (1990-the year the map recommended). Each observation is a 30×30m pixel. Optimal bandwidth is calculated as in Calonico et al. (2014) and using a triangular weighting kernel. Housing development is an indicator, equals one if a building developed during 2008-2020, otherwise zero. Terrain characteristics include slope, roughness, and Terrain Ruggedness Index. Taxable improved property values are missing in three counties: Contra Costa, Montery, Shasta, thus they are excluded in the sample used in columns (4)-(6). Standard errors are clustered at city level.

*** p<0.01, ** p<0.05, * p<0.1

Table A2: Placebo Test: terrain characteristics

	Slope (1)	Roughness (2)	Terrain Ruggedness Index (3)
Inside VHFHSZ	0.100	0.154	-0.064
	(0.297)	(0.455)	(0.747)
City fixed effects	Yes	Yes	Yes
Dependent variable mean	7.434	13.379	20.501
Bandwidth (meters)	119	115	126
Observations	654,942	625,197	700,737

Notes: This table presents RD regression results of terrain characteristics. Each observation is a 30×30m pixel. Optimal bandwidth is calculated as in Calonico et al. (2014) and using a triangular weighting kernel. Standard errors are clustered at city level.

*** p<0.01, ** p<0.05, * p<0.1

Table A3: Spatial Regression Discontinuity Estimates: robustness check using taxable improved property value

	(1)	(2)	(3)
Inside VHFHSZ	-3769.153*	-3803.870*	-2259.549*
	(2098.641)	(2094.298)	(1290.065)
Terrain characteristics		Yes	Yes
City fixed effects			Yes
Dependent variable mean	6610.262	6610.262	6610.262
Bandwidth (meters)	193	193	193
Observations	1,013,222	1,013,222	1,013,222

Notes: Each observation is a 30×30m pixel. Optimal bandwidth is calculated as in Calonico et al. (2014) and using a triangular weighting kernel. Taxable improved property values are missing in three counties: Contra Costa, Montery, Shasta, thus they are excluded in the sample. Standard errors are clustered at city level.

*** p<0.01, ** p<0.05, * p<0.1

Table A4: Permutation Test

	60m (1)	90m (2)	120m (3)	150m (4)	180m (5)
Panel [A]: Housing development	-0.000	-0.001	-0.001	0.002**	-0.001
	(0.001)	(0.001)	(0.001)	(0.001)	(0.001)
Panel [B]: Log(taxable improved property value)	0.003	-0.002	-0.005	0.010	-0.006
	(0.020)	(0.010)	(0.010)	(0.010)	(0.010)
Terrain characteristics	Yes	Yes	Yes	Yes	Yes
City fixed effects	Yes	Yes	Yes	Yes	Yes

Notes: Each observation is a 30×30m pixel. Optimal bandwidth is calculated as in Calonico et al. (2014) and using a triangular weighting kernel. Each cell is a separate RD regression. Each column represents moving the boundary outside the true boundary with a certain distance, for example, 30m indicates that the boundary is moved outside the true boundary 30 meters. Standard errors are clustered at city level.

*** p<0.01, ** p<0.05, * p<0.1

A14

B Data appendix

B.1 Taxable improved property value at pixel level

Taxable improved property value is from parcel data. I use the improvement value of the parcel to indicate the taxable property value. Among the sixteen counties covered in this study, the value is missing in three counties: Contra Costa, Montery, Shasta. I reorganize it at pixel level for analysis. I first perform a GIS intersection between parcels and pixels. I get which parcels each pixel intersects, and the overlapped area. Figure B1 presents an example of the intersection. I then calculate the overlap ratio by dividing the overlapped area over the corresponding parcel area. Thus I get how much of each parcel that intersects the pixel. Multiplying each ratio with the property value, and then summing up to the pixel, then I get the weighted property value at pixel level. Our main analysis focuses on 2008-2020. I calculate the weighted property value for all parcels built during 2008-2020.[23] In our identification test, I also use the weighted property value for all parcels built before 2008 (1990-2007).

Housing development is an indicator based on whether a 2008-2020 developed building intersects the pixel. If true, then the pixel is assigned one for the outcome, otherwise zero. The same logic applies to pre-period (1990-2007) development.

B.2 Cities and terrain characteristics

B.2.1 Cities

To determine the city each pixel located, I collected the GIS data of all California incorporated cities.[24] Then I use GIS software to intersect each pixel centroid with the city GIS file. For pixels outside the incorporated cities, I consider it within incorporated areas, and assign an unique id to it in the corresponding county.

B.2.2 Terrain characteristics

Terrain characteristics in our sample include slope, roughness and Terrain Ruggedness Index (TRI). Slope is the angle of inclination of the terrain and is expressed in degrees. Roughness

---

[23]I use the "built year" characteristic for each parcel to determine the built time of development.

[24]Data is from CAL FIRE: https://data.ca.gov/dataset/california-incorporated-cities. There are 482 cities in the data.

is computed from the elevation. It's the degree of irregularity of the surface. TRI summarizes the change in elevation within the 3×3 pixel grid, and is a measurement of terrain heterogeneity. All of three indexes are from the National Land Cover Database (NLCD) 2006, when is the pre-treatment period. There are originally in raster format, and I convert them to vector format for further GIS use. Each index is originally at 30×30m pixel level.

B.3 Local government finance data

Our sample covers 277 cities and unincorporated areas in sixteen counties in California. I take several steps to create the property tax dependency index and match it with pixel level data.

B.3.1 Creating property tax revenue dependency index

I use the Government Finance Database (GFD, Pierson et al., 2015) for the source of financial data at local government level. I restrict the data to counties, municipalities, and townships in California and year 2007.

I create the property tax revenue dependency index by using "total property tax revenue/(total revenue-total property tax revenue)", i.e. the share of total local government revenue that comes from property tax compared to all other sources (sales tax, excise tax, etc.). For incorporated cities, I directly create this index at the city level. I also create the same index at the county level, which is used to proxy for the value in unincorporated areas.

With the property tax revenue dependency index at the local government level, I find the median value and define a dummy variable for each city and county, which equals one if the index is above the median value, and zero if it's equal or below the median value.

B.3.2 Matching local governments

Each pixel in the sixteen counties is located in either a city/township or unincorporated areas in the county. I use the GIS software to determine this location. Then for all pixels, we know which city/township/county that they are located in.

I match the pixel level data with the property tax revenue dependency data by matching the city/township name. All 277 cities are successfully matched. For pixels that are located in unincorporated areas, I match them to the dependency index at the county level. Around 66.3% of the pixels are located in areas with a high property tax revenue dependency index.

Figure B1: Intersection between parcels and pixels
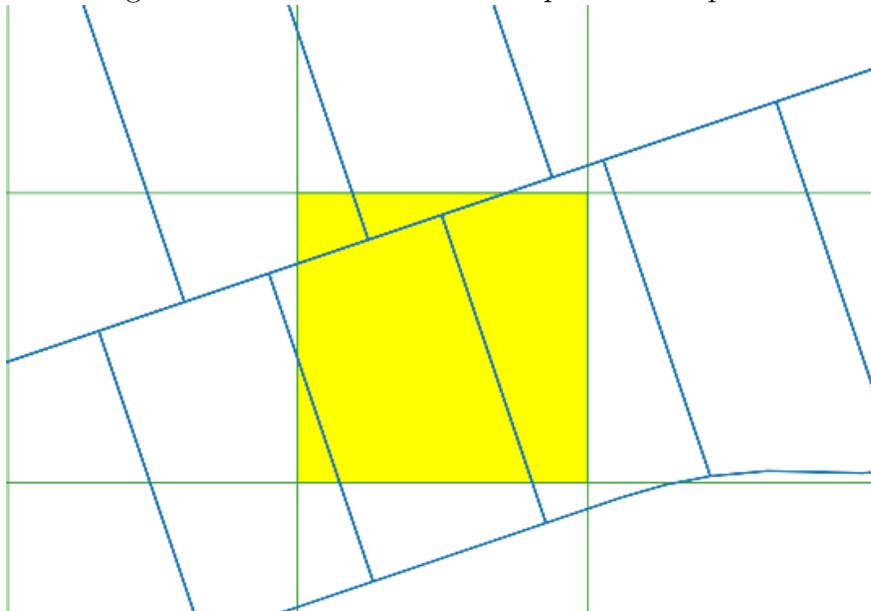
Notes: The square with green boundary is a pixel. The polygons with blue boundaries are parcels. The highlighted pixel intersects five parcels.

C   Appendix: Fire Hazard Severity Zone Methods

This appendix provides details on how the Fire Hazard Severity Maps are drawn, based on the materials provided by CAL FIRE. Fire hazard severity zone (FHSZ) is designated to reflect the fire hazard potential over the long term for all areas of California. The zones reflect areas with similar burn probabilities and fire behavior. There are three classes: moderate, high and very high. In LRA, only very high FHSZs are designated. The designation of wildland areas and non-wildland areas. Wildland areas are modeled directly using the fuel model and data inputs within the wildland, while non-wildland areas are modeled based on the proximity to wildland areas and the probability of fire spread from wildland areas. Basically, there are five modules in the process.

C.1   Module 1 - Delineate wildland zone polygons

The first step is to divide wildland areas into zone polygons with similar fire behavior potential. The inputs are vegetation type, slope and watershed boundaries. No maximum size of the zone, but there is a minimum size of 200 acres in wildland. Figure C1 shows this process.

Figure C1: FHSZ Method - Module 1
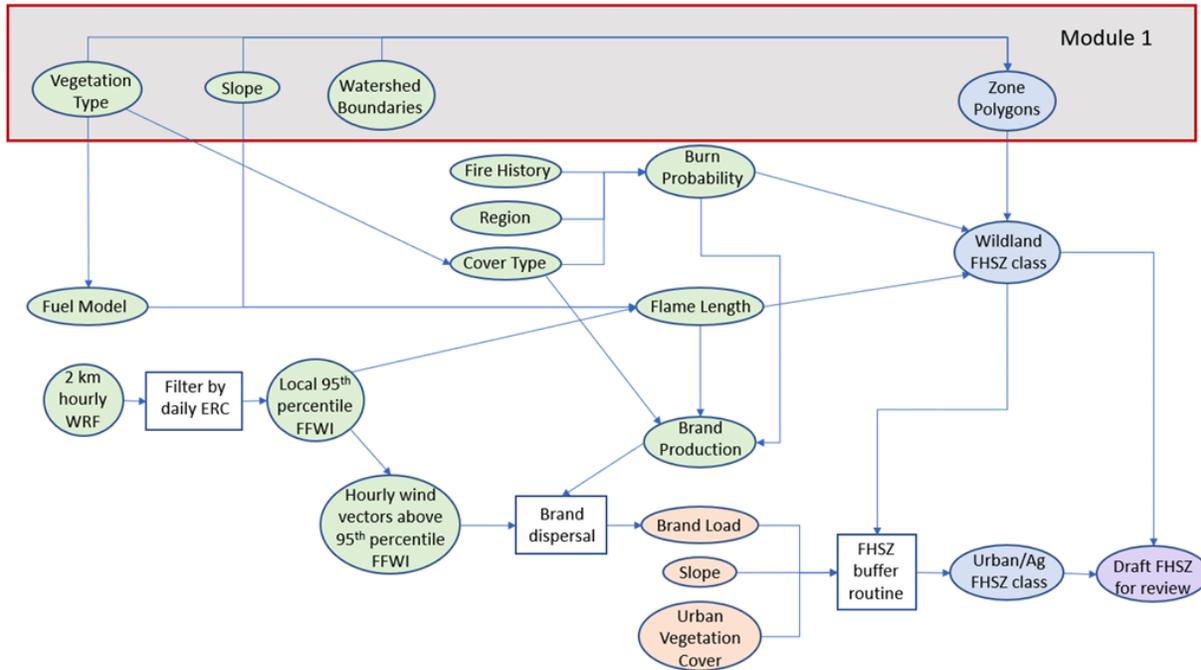
Notes: Provided by CAL FIRE.

C.2 Module 2 - Wildland FHSZ classification

Each zone is assigned a hazard score, which is calculated by multiplying flame length and burn probability. The flame length is the expected one under the worst conditions based on several fuel models and at the 30 meter pixel scale. Burn probability is the inverse of fire rotation, which is calculated using fire history for the last 30-50 years. Burn probability is at a different scale from flame length, which is the strata level. With the flame length at 30 meter pixel level and burn probability at strata level, then each 30 meter pixel receives hazard score. The hazard score of each zone polygon is averaged from all pixels within it. The zone score is then classified into three classes: moderate, high, and very high. Figure C2 shows this process.

Figure C2: FHSZ Method - Module 2
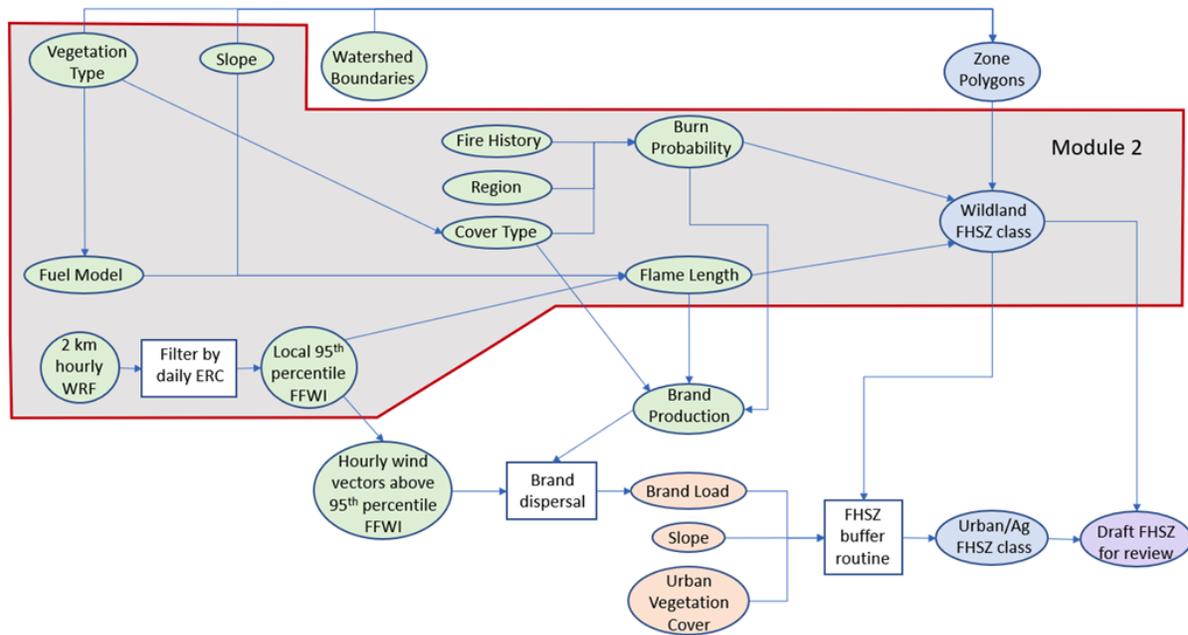
Notes: Provided by CAL FIRE.

C.3   Module 3 - Fire brand production and dispersal

This module calculates estimates using for FHSZ classification in non-wildland areas. The first is to calculate the potential fire brands produced at each 30 meter pixel. It is mainly based on vegetation type, flame length, and burn probability. Then it models the dispersal of the fire brand based on the direction and speed of the wind in the area. A higher speed will disperse the fire brand at greater distance into non-wildland areas. The final fire brands for a non-wildland area is the sum of all previous wildland pixels. Figure C3 shows this process.

Figure C3: FHSZ Method - Module 3
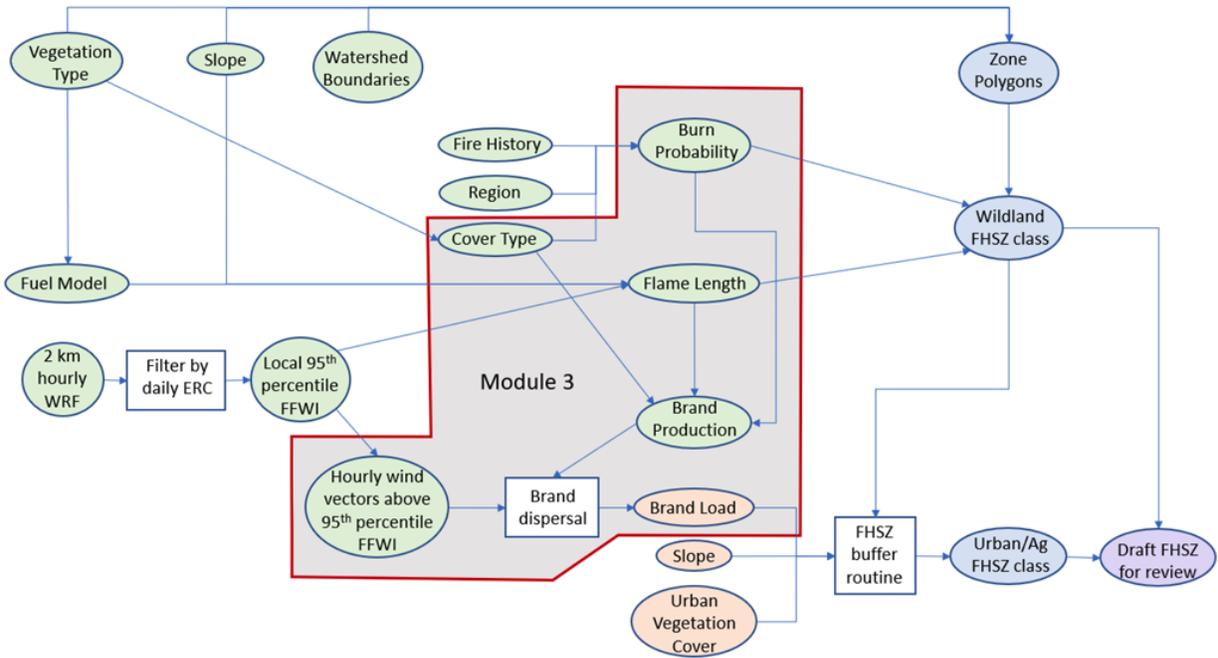
Notes: Provided by CAL FIRE.

C.4 Module 4 - Non-wildland FHSZ classification

A buffer is created from the wildland boundary into the non-wildland areas. The width of the buffer is determined by the modeled brand load, slope, and the tree cover. For example, the buffer will be wider if the areas have higher brand load, steeper slope and greater tree cover. The zone hazard class in the non-wildland areas is the same as the adjacent wildland, and the classification takes the one from the buffer of lower FHSZ classes for further distances. Only the buffers within non-wildland areas are classified, which is different from wildland areas that all of the areas receive a hazard classification.

Figure C4: FHSZ Method - Module 4
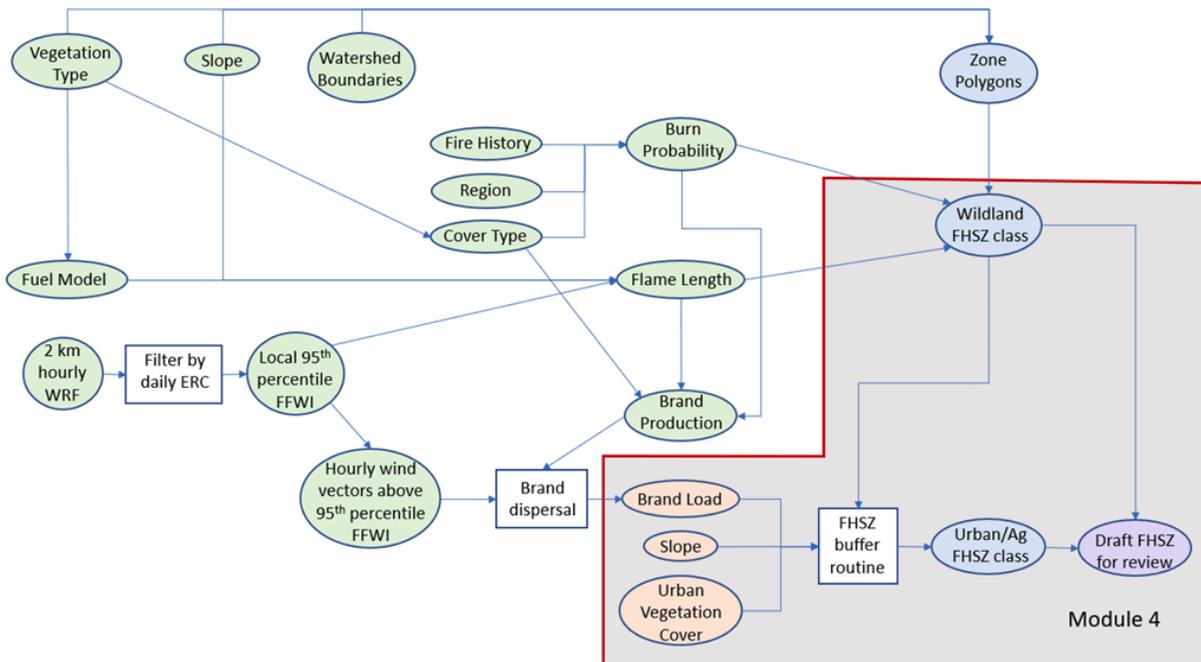
Notes: Provided by CAL FIRE.

C.5 Module 5 - Finalizing maps

The zones in wildland areas and non-wildland areas are intersected with State Responsibility Areas (SRA) and Local Responsibility Areas (LRA). For SRA, all unzoned areas are designated moderate classification to satisfy the statute requirement that all SRA should be hazard-classified.

For LRA, CAL FIRE recommend the maps to local jurisdictions. The local juridiction usually hold a local review for the maps. The review process vary on a case-by-case basis. Some cities hold public forums while others may just provide the information on websites. For example, Newport Beach City in Orange County posted a public notice on the city official website stating that "This notice is provided pursuant to Government Code Section 51178.5 and requires the City of Newport Beach to make this information available for view in a format that is understandable and accessible to the general public." Per law, local governments have 120 days to decide to adopt or reject the maps.